Chemical Geology 256 (2008) 172–184

Contents lists available at ScienceDirect

Chemical Geology

journal homepage: www.elsevier.com/locate/chemgeo

Partitioning of Cl and F between fluid and hydrous phonolitic melt of Mt. Vesuvius at ~850–1000 °C and 200 MPa

Vitaliy Yu. Chevychelov [a,*], Roman E. Botcharnikov [b], Francois Holtz [b]

[a] Institute of Experimental Mineralogy, Russian Academy of Sciences, Chernogolovka, Moscow oblast, 142432, Russia
[b] Institut fur Mineralogie, Leibnitz Universitat Hannover, Callinstr. 3, D-30167, Hannover, Germany

ARTICLE INFO

Article history:
Received 20 December 2007
Received in revised form 27 May 2008
Accepted 18 June 2008

Keywords:
Fluorine
Chlorine
Mixed fluid
Partitioning
Phonolitic melt
Vesuvius volcano

ABSTRACT

The solubilities of Cl- and/or F-bearing fluids in phonolitic melts of Vesuvius volcano have been determined experimentally at temperatures of 845–865 °C and 1000 °C, and pressure of 200 MPa. At 845–865 °C, the maximum Cl concentration in the melt (^{m}Cl) coexisting with Cl-rich (~35.5 wt.%; ^{fl}Cl) and F-free fluid is about 0.5 wt.%. An addition of F to the system increases the Cl content of the melt up to 0.7 wt.% at ~39 wt.% Cl and ~13 wt.% F in the fluid(s). The relationship between ^{m}Cl and ^{fl}Cl indicates that low-density vapor and dense brine phases might have coexisted in some experiments. The relationship between ^{m}Cl and ^{fl}Cl at 1000 °C is similar to that determined at 845–865 °C, implying that variations of temperature in the range 850–1000 °C have no significant effect on the partitioning of Cl between fluid and phonolitic melt.

The concentration of F in phonolitic melt coexisting with F-rich fluid(s) reaches at least 0.9 wt.% at 845–865 °C and 1.3 wt.% at 1000 °C. The comparison of data from experiments conducted in Au and Pt capsules indicates that F may react with Au, which influences the quality of the experimental results. The partition coefficients of F between bulk fluid and melt ($^{fl/m}D_F$) are higher than 1 in all experiments, indicating that fluorine is preferentially incorporated into the fluid phase in phonolitic systems, in contrast to $^{fl/m}D_F$ values determined in rhyolitic systems. The influence of Cl on $^{fl/m}D_F$ is not detectable at the conditions of our experiments. The experimental data imply that Mt. Somma–Vesuvius phonolitic magmas from the eruptions between A.D. 79 and A.D. 1944 may have coexisted with Cl-rich and F-rich fluid phase(s) prior to eruption.

1. Introduction

Knowledge on the solubility of volatiles in natural magmatic melts of different composition and on the partitioning of volatiles between fluid and melt is of fundamental importance for understanding and modeling of magma degassing processes at active volcanoes. Chlorine and fluorine are only minor volatile components in typical natural magmas and, except for few systems, they do not have a significant influence on their properties (e.g., on melt viscosity, melt density and crystallization temperature). On the other hand, both volatile components may be present in significant amounts in magmatic gases and may have an effect on the properties of the exsolving fluid phase (e.g., fluid immiscibility, e.g., Ravich, 1974; Shinohara et al., 1989; Carroll and Webster, 1994; Shinohara, 1994; Webster et al., 1999; Kotelnikova and Kotelnikov, 2002; Veksler, 2004; Thomas et al., 2005; Webster & Mandeville, 2007; Stelling et al., 2008-this issue) as well as on the efficiency of metal transport in magmatic/hydrothermal fluids (e.g., Marakushev et al., 1983; Candela and Piccoli, 1995; Thompson et al., 2007; Heinrich, 2007).

The Cl content of aluminosilicate melt is dependent on the Cl/H_2O ratio of the coexisting fluid phase (e.g., Webster, 1997a; Webster and Rebbert, 1998; Webster et al., 1999; Chevychelov et al., 2003; Webster, 2004). Experimental studies on the solubility of H_2O–Cl-bearing fluids in silicate melts show that Cl typically partitions in favor of aqueous fluids rather than silicate melts (e.g., Koster van Groos and Wyllie, 1969; Kilinc and Burnham, 1972; Malinin et al., 1989; Shinohara et al., 1989; Métrich and Rutherford, 1992; Webster, 1992a,b; Carroll and Webster, 1994; Kravchuk and Keppler, 1994; Gorbachev, Khodorevskaya, 1995; Malinin and Kravchuk, 1995; Webster, 1997a,b; Chevychelov, 1999; Webster et al., 1999; Signorelli and Carroll, 2000, 2002; Webster and De Vivo, 2002; Chevychelov and Suk, 2003; Chevychelov et al., 2003; Botcharnikov et al., 2004; Carroll, 2005; Mathez and Webster, 2005; Botcharnikov et al., 2007; Stelling et al., 2008-this issue). At a given fluid composition, the molar Al/(Na+K) ratio of the melt has a large effect on Cl concentration in hydrous felsic melts, with a concentration minimum at Al/(Na+K)=1 (Métrich and Rutherford, 1992; Webster, 1992b; Chevychelov, 1999; Carroll, 2005). In brine-saturated igneous systems under conditions of geological interest, maximum Cl concentrations can reach up to ~1–1.5 wt.% in hydrous felsic melts and increase up to ~3–5.9 wt.% in hydrous basaltic melts

* Corresponding author. Institute of Experimental Mineralogy, Russian Academy of Sciences, ul. Institutskaja 4, Chernogolovka, Moscow oblast, 142432, Russia.
E-mail addresses: chev@iem.ac.ru (V. Yu. Chevychelov), rbotcharnikov@yahoo.com (R.E. Botcharnikov).

0009-2541/$ – see front matter © 2008 Elsevier B.V. All rights reserved.
doi:10.1016/j.chemgeo.2008.06.025

(Chevychelov, 1999; Mathez and Webster, 2005; Webster et al., 1999; Webster and De Vivo, 2002; Chevychelov and Suk, 2003; Stelling et al., 2008-this issue).

Temperature and pressure may also influence the concentration of Cl dissolved in a silicate melt. For instance, an increase in experimental temperature from 800 to 1000 °C or a decrease in pressure from 500–800 to 100–200 MPa at low Cl content (1–2 M) in the coexisting fluid can enhance Cl concentration in subaluminous granitic melts up to by a factor of 2–3 (Webster, 1992a; Chevychelov and Chevychelova, 1997). However, the temperature and pressure dependence of Cl solubility is strongly controlled by the melt composition.

Reported experimental data on the solubility of F–H_2O-bearing fluids in melts of predominantly rhyolitic composition (saturated and under-saturated in F-bearing mineral phase) indicate that concentrations of dissolved F can exceed 10 wt.%, especially in felsic melts (e.g., Koster van Groos and Wyllie, 1968; Kovalenko, 1977; Glyuk et al., 1980; Manning, 1981; Webster, 1990; Webster and Holloway, 1990; Keppler and Wyllie, 1991; Holtz et al., 1993; Keppler, 1993; Carroll and Webster, 1994; Price et al., 1999; Kravchuk and Slutsky, 2001; Scaillet and Mcdonald, 2003, 2004; Chevychelov et al., 2005; Gabitov et al., 2005; Gramenitskiy et al., 2005; Dolejs and Baker, 2006, 2007a,b; Lukkari and Holtz, 2007). In fluid-saturated magmatic systems, the partition coefficient of F between fluid and melt ($^{fl/m}D_F$) ranges from 0.2 to >1.0. In a system composed of fluid and topaz rhyolite melt, D_F increases strongly with temperature and F content (Webster and Holloway, 1990; Webster, 1990). Rhyolitic quartz-normative melts can dissolve less fluorine than nepheline-normative compositions. For subaluminous melts, there are two F concentration maxima near quartz–albite and albite–nepheline eutectics (Gramenitskiy et al., 2005). The concentration of F exhibits a minimum near metaluminous rhyolitic compositions and measurably increases in peraluminous and peralkaline (especially Na-rich) melts (e.g., Scaillet and Mcdonald, 2004; Gramenitskiy et al., 2005; Dolejs and Baker, 2006; Lukkari and Holtz, 2007). The solubility of water increases with fluorine content of the silicate melt (Kovalenko, 1977; Holtz et al., 1993; Dolejs and Baker, 2007b). The effects of T and P on F concentration in the silicate melt are not well constrained (Carroll and Webster, 1994). For instance, early experiments show that as T increases from 550 to 800 °C at P=50–100 MPa, the F contents of ongonitic melts remain constant at low (0.7–1.0 wt.%) bulk F contents in the melt–fluid system and increase in case of higher (3.0–3.3 wt.%) bulk F contents (Kovalenko, 1977). Recent studies, using hydrous haplogranitic melts at 100 MPa, show a positive temperature dependence of fluorite solubility (Gabitov et al., 2005; Dolejs and Baker, 2006).

Chlorine and fluorine are typical volatile components present in most fluid-bearing felsic alkali-rich silicate melts like phonolites and pantellerites (e.g., Christiansen and Lee, 1986; Dunbar et al., 1989; Lowenstern, 1994; Harms and Schmincke, 2000; Straub and Layne, 2003). However, there are only few experimental data on the solubility of complex H_2O–Cl–F-bearing fluids in silicate melts and on the partitioning of F and Cl between fluids and melts (Webster, 1990; Webster and Holloway, 1990; Webster and Rebbert, 1998). The obtained results indicate that Cl concentration in melts increases with increasing F contents (Webster, 1997a; Webster and Rebbert, 1998) in rhyolitic melts. To our knowledge, there are no systematic experimental data which can be applied to phonolitic systems. Although in the experiments of Signorelli and Carroll (2000, 2002) on Cl partitioning between fluid and melt natural phonolite containing about 0.4 wt.% F was used as a starting material, the concentrations of F in the experimental products were not reported.

This study is focused on the solubility of Cl- and F-bearing aqueous fluids in a phonolitic melt of Mt. Vesuvius. Phonolitic magmas of Mt. Vesuvius contain mainly H_2O, F, Cl, and, to a lower extent, S, CO_2, B (e.g., Santacroce et al., 1993; Marianelli et al., 1995; Belkin et al., 1998; Marianelli et al., 1999; Signorelli and Capaccioni, 1999; Signorelli et al., 1999; Cioni, 2000; Raia et al., 2000; Paone et al., 2001; Webster et al., 2001; Webster and De Vivo, 2002; Lima et al., 2007), providing an ideal example of a Cl–F-bearing magmatic system. An additional advantage is that the solubility of H_2O–Cl-bearing fluids in phonolites of Mt. Vesuvius has been already investigated by Signorelli and Carroll (2000), giving independent reference dataset. We present new experimental results obtained at 200 MPa allowing us to determine the solubility of Cl–F–H_2O-bearing fluids in phonolitic melts and the resulting partition coefficients of Cl and F between fluid and melt.

2. Experimental and analytical methods

2.1. Starting materials

The starting material was a synthetic analogue of a phonolite (Table 1, "A"), which corresponds to the K-rich sample of a phonolitic pumice collected from the fallout deposit of the 79 A.D. eruption of Vesuvius (Signorelli and Carroll, 2000). A gel was prepared from a mixture of chemical reagents (CaO, MgO, $Al(NO_3)_3$, $NaNO_3$, KNO_3, carbonyl Fe, and $C_8H_{20}O_4Si$ solution), following the standard procedures described by Roy (1956) and Hamilton and Henderson (1968). The final annealing temperature was 600 °C. This starting composition labeled "B" in Table 1 was used for all experiments at T=1000 °C and for 4 experiments at T~850 °C (Table 2) to avoid crystallization of mica (biotite). The composition "A" was prepared by adding TiO_2 and MnO to the gel "B". This mixture was heated stepwise from 600 to 800 °C in air at 1 atm for 31 h. The starting material "A" was used for experiments at T~850 °C (except 4 experiments, see above). The starting powders were stored in a desiccator to minimize adsorption of atmospheric H_2O.

2.2. Experiments

The mixture of starting material (25–50 mg) and an aliquot (2.5–7.5 mg) of aqueous (HCl+HF), HCl, HF solutions [with (HCl+HF) concentration of 1–16 mol/kg] or pure water were loaded in 15-mm-long (inner diameter of 2.8 mm) Au or $Au_{80}Pd_{20}$ (used only for 5 experiments at 845–865 °C) capsules. Two series of experiments at 1000 °C has been conducted in Au and Pt capsules in order to check whether capsule material may affect the high temperature experimental results (see discussion below). The loaded masses of phonolitic mixture and of solution are given in Table 2. The aqueous solutions used in experiments have been prepared from initial 33 wt.% HCl and 48 wt.% HF solutions. Exact concentrations of Cl and F in those solutions were verified by a titration method using standard 1 N solution of NaOH (with high-precision weighing at

Table 1
Chemical composition of starting mixtures of phonolitic composition in wt.%

Number	SiO_2	TiO_2	Al_2O_3	FeO_{tot}	MnO	MgO	CaO	Na_2O	K_2O	Total	A/CNK[a]	A.I.[b]	N/NK[c]
A	57.36	0.18	21.72	2.23	0.12	0.23	2.94	5.69	9.54	100.01	0.87	0.91	0.48
B	57.53	–	21.79	2.24	–	0.23	2.95	5.70	9.56	100	0.87	0.91	0.48

[a] Molar $Al_2O_3/(CaO+Na_2O+K_2O)$ ratio.
[b] Agpaitic index=Molar $(Na_2O+K_2O)/Al_2O_3$ ratio.
[c] Molar $Na_2O/(Na_2O+K_2O)$ ratio.

Table 2
Conditions, starting mass relations, and fluid compositions in the experimental runs at P=200 MPa

Run number	Duration (h)	T (°C)	Mass starting phonolitic powder (mg)	Starting solution		f_{O2}	Solution/powder[a]
				Composition (wt.%)	Mass (mg)		
PG-13	205	855	35.96	H_2O	5.78	NNO	0.16
PG-61[b]	180	865	28.08	H_2O	4.67	NNO	0.17
PG-56[c]	179	865	24.77	3.9 HCl	2.64	NNO	0.11
PG-55[c]	179	865	25.47	11.2 HCl	2.60	NNO	0.10
PG-54[c]	179	865	24.83	23.7 HCl	2.50	NNO	0.10
PG-49	168	865	48.53	2.0 HF	4.85	NNO	0.10
PG-28	168	855	43.95	4.5 HF	6.37	NNO	0.14
PG-45	189	865	48.70	5.9 HF	5.48	NNO	0.11
PG-27	168	855	31.06	10.3 HF	4.42	NNO	0.14
PG-53	168	865	48.73	13.0 HF	4.72	NNO	0.10
PG-48	168	865	47.16	3.9 HCl+2.0 HF	4.98	NNO	0.11
PG-60[b]	180	865	28.12	2.6 HCl+4.0 HF	4.40	NNO	0.16
PG-25	174	855	24.92	3.5 HCl+5.4 HF	3.93	NNO	0.16
PG-12	205	855	40.91	4.0 HCl+8.4 HF	5.66	NNO	0.14
PG-16	175	850	34.77	4.2 HCl+8.2 HF	4.64	NNO	0.13
PG-39	186	865	49.24	3.9 HCl+13.0 HF	6.40	NNO	0.13
PG-46	189	865	49.27	11.2 HCl+2.0 HF	5.87	NNO	0.12
PG-59[b,c]	179	865	27.74	7.5 HCl+3.9 HF	4.81	NNO	0.17
PG-11	205	855	28.65	9.1 HCl+9.2 HF	4.73	NNO	0.17
PG-52	168	865	48.60	11.2 HCl+13.1 HF	5.16	NNO	0.11
PG-9	170	845	45.73	15.4 HCl+5.6 HF	7.54	NNO	0.17
PG-8	170	845	34.74	15.7 HCl+9.0 HF	5.74	NNO	0.17
PG-58[b,c]	179	865	28.51	19.5 HCl+1.6 HF	4.26	NNO	0.15
PG-41	186	865	49.91	23.7 HCl+2.0 HF	6.19	NNO	0.12
PG-40	186	865	48.61	23.2 HCl+6.3 HF	6.63	NNO	0.14
PG-51	168	865	46.81	23.9 HCl+12.7 HF	5.50	NNO	0.12
PR-72[b,d]	120	1000	50.43	H_2O	6.81	~NNO+3.5	0.13
PR-70[b,d]	120	1000	50.33	3.7 HCl	6.87	~NNO+3.5	0.14
PR-66[b,d]	120	1000	50.11	11.1 HCl	7.29	~NNO+3.5	0.15
PR-60[b,d]	120	1000	50.11	23.9 HCl	7.50	~NNO+3.5	0.15
PR-71[b,d]	120	1000	47.90	2.0 HF	6.92	~NNO+3.5	0.14
PR-68[b,d]	120	1000	50.48	5.8 HF	6.99	~NNO+3.5	0.14
PR-63[b,d]	120	1000	50.40	13.4 HF	7.24	~NNO+3.5	0.14
PR-69[b,d]	120	1000	50.35	3.8 HCl+1.9 HF	7.13	~NNO+3.5	0.14
PR-67[b,d]	120	1000	50.18	3.7 HCl+5.6 HF	7.20	~NNO+3.5	0.14
PR-62[b,d]	120	1000	50.09	3.7 HCl+13.2 HF	7.14	~NNO+3.5	0.14
PR-65[b,d]	120	1000	50.05	11.1 HCl+1.9 HF	7.32	~NNO+3.5	0.15
PR-64[b,d]	120	1000	50.08	11.1 HCl+5.6 HF	7.40	~NNO+3.5	0.15
PR-61[b,d]	120	1000	50.14	10.9 HCl+12.8 HF	7.45	~NNO+3.5	0.15
PR-59[b,d]	120	1000	50.03	23.5 HCl+1.8 HF	7.62	~NNO+3.5	0.15
PR-58[b,d]	120	1000	50.01	23.3 HCl+5.1 HF	7.20	~NNO+3.5	0.14
PR-57[b,d]	120	1000	50.06	23.0 HCl+11.3 HF	6.97	~NNO+3.5	0.14
PG-72[b]	144	1000	26.88	H_2O	2.58	~NNO+3.5	0.10
PG-77[b]	144	1000	26.86	3.9 HCl	3.20	~NNO+3.5	0.12
PG-73[b]	144	1000	27.21	11.2 HCl	3.39	~NNO+3.5	0.12
PG-78[b]	144	1000	27.30	2.0 HF	3.01	~NNO+3.5	0.11
PG-80[b]	144	1000	26.84	5.9 HF	3.18	~NNO+3.5	0.12
PG-67[b]	144	1000	27.03	13.0 HF	2.82	~NNO+3.5	0.10
PG-79[b]	144	1000	26.83	3.9 HCl+2.0 HF	3.20	~NNO+3.5	0.12
PG-81[b]	144	1000	27.21	3.9 HCl+5.9 HF	3.00	~NNO+3.5	0.11
PG-75[b]	144	1000	26.99	3.9 HCl+13.0 HF	2.78	~NNO+3.5	0.10
PG-82[b]	144	1000	27.53	11.2 HCl+2.0 HF	3.21	~NNO+3.5	0.12
PG-74[b]	144	1000	27.08	11.2 HCl+5.9 HF	3.37	~NNO+3.5	0.12
PG-68[b]	144	1000	27.03	11.2 HCl+13.1 HF	2.77	~NNO+3.5	0.10
PG-70[b]	144	1000	27.07	23.2 HCl+6.3 HF	2.80	~NNO+3.5	0.10
PG-71[b]	144	1000	27.21	23.9 HCl+12.7 HF	2.34	~NNO+3.5	0.09

[a]Starting solution/phonolitic powder ratio by weight before the run.
[b]All the experiments were done with starting material — "A" (Table 1) except those marked with ([b]) done with starting material — "B".
[c,d]All the experiments were done in Au capsules except those marked with ([c]) done in $Au_{80}Pd_{20}$ capsules, and with ([d]) done in Pt capsules.

all stages). The initial ratio of aqueous solution to phonolitic glass powder in the capsules was kept low (0.1–0.2 by weight; Table 2) in order to minimize the incongruent dissolution of silicate components in the coexisting fluid phase during the experiment. The amount of added aqueous fluid was sufficient to ensure fluid saturation of the phonolitic melt at the experimental conditions. Capsules were welded shut and heated overnight in an oven at 110 °C to ensure fluid homogenization throughout the charge and to check for leaks.

At 845–865 °C, the experiments were carried out in conventional horizontal externally heated cold seal pressure vessels (CSPV) made of a nickel-based alloy. The vessels were pressurized with water. The oxygen fugacity inside CSPVs was buffered through the reaction of water with the Ni/NiO solid oxygen buffer (charged as a mixture of Ni and NiO powders, NNO). The use of water as the pressure medium and the nickel-based alloy of the vessel allowed us to keep the f_{O2} conditions at the NNO for the duration of the experiment in the CSPVs. The temperature was controlled with an external Ni–CrNi thermocouple (vessels are calibrated for

temperature) and the variations were less than 5 °C. Pressure was measured with a pressure transducer calibrated against a strain gauge manometer and controlled manually. The pressure variations were less than 5 MPa. The experimental runs were quenched isobarically by removing the furnace from the vessel and using a flux of compressed air around the vessel (quench rate is about 200 K/min).

At 1000 °C, the experiments were conducted in two internally heated pressure vessels (IHPV) pressurized with pure Ar gas. Experiments with Au capsules have been conducted at Hannover (Berndt et al., 2002). The capsules were placed in the vessel, pressurized to 200 MPa and isobarically heated up to the desired temperature of the experiment. The temperature was monitored with three sheathed K-type thermocouples with an uncertainty of ±5 °C. Total pressure was controlled with a Burster Type 8221 transducer (pressure uncertainty is ±1 MPa). Pressure variations during the experiment were less than 5 MPa. In these experiments, oxygen fugacity in the capsules was controlled by the intrinsic redox conditions of the IHPV and by a diffusion of H_2 through capsule walls at high *T*. Thus, the oxygen fugacity of water-saturated runs was close to log f_{O2} ~ NNO + 3.5 (Berndt et al., 2005). The experiments were quenched isobarically by switching off the power supply of the furnace. The initial quench rate was about 200 K/min. All experiments in Pt capsules have been performed at the Institute of Experimental Mineralogy, Chernogolovka. The working conditions were analogous to that of the IHPV in Hannover, except that temperature was measured by four S-type thermocouples along a 35-mm zone. Pressure was measured and controlled using both pressure transducer and manometer. The quench rate was also close to 200 K/min.

It must be noted that the quench rates in both CSPV and IHPVs were sufficient to prevent formation of quench crystals in K-rich melts (no quench minerals could be identified using electron microprobe). However, some experimental glasses, in particular in Cl- and F-rich systems, contained tiny bubbles (<1 μm in diameter) which were presumably formed during quench.

The run duration of the experiments was 168 to 205 h (7 to 8.5 days) at 845–865 °C and 120 h in Pt and 144 h in Au capsules at 1000 °C (Table 2). Previous studies have shown that a duration of 2–5 days is sufficient to achieve equilibrium partitioning of Cl between felsic melts and fluids at conditions similar to our experiments (e.g., Malinin et al., 1989; Shinohara et al., 1989; Métrich and Rutherford, 1992; Webster, 1992a; Chevychelov, 1999). In the case of the Vesuvius phonolite, the attainment of equilibrium required less than 6 days at 100 MPa and 870 °C (Signorelli and Carroll, 2000). Therefore, the run duration applied in our study was long enough to approach equilibrium conditions at temperatures above 840 °C.

After the experiment, the capsules were removed from the pressure vessels, dried and weighed to check for leaks. Capsules showing anomalous weight changes were discarded. Capsules from successful runs were pierced with a needle and put in an oven at 110 °C for 3 min. Then, the capsules were reweighed to determine the total amount of evaporated solution. Afterwards, capsules were open with pliers and fragments from each sample were mounted in epoxy resin. The experimental glasses were prepared as polished thin sections for petrographic and electron microprobe analyses.

2.3. Electron microprobe analyses

The run products were composed of glass and minerals (biotite, plagioclase, clinopyroxene at 845–865 °C; Table 3). A Cameca SX-100 electron microprobe and CamScan MV2300 electron microscope with X-ray spectrometer (for all samples in Pt capsules) were used to identify the minerals and to analyze the composition of the glasses. Glass analyses, using Cameca SX-100 electron microprobe, were conducted with 15 kV acceleration potential, 4 nA beam current, a defocused electron beam (10–20 μm diameter), and peak counting times of 2–8 s (for major elements). Sodium and potassium were analyzed for 2 s to minimize their migration. No corrections for possible alkali loss during glass analysis were made. However, from our experience we do not expect significant problem due to alkali loss with our analytical conditions (e.g., Freise et al., 2003; Botcharnikov et al., 2004; Stelling et al., 2008-this issue). Chlorine and fluorine were measured as the last elements, using a 15 nA beam current and counting times of 30 s for F, and 30 nA beam current and counting times of 30 and 60 s for Cl. Standards for F and Cl were apatite (3.53 wt.% F) and NaCl, respectively. Using such analytical conditions, the detection limit of Cl was ~100 ppm and the detection limit of F was ~1000 ppm. The analyses of Cl and F in glasses from Pt capsules were performed with CamScan MV2300 electron microscope at 15 kV acceleration potential, 11–16 nA beam current with a scanning area of about 50×50 μm. The counting times were 30 s for F and 20 s for Cl. CaF_2 and NaCl crystals were used as standards for F and Cl, respectively. Major-element composition was determined using an EDX system combined with CamScan MV2300 electron microscope. It must be noted that the presence of Fe in a silicate glass may affect the analysis of F due to overlapping of the Kα line of F with Lα and Ll lines of Fe. To avoid or minimize the interferences between these two elements, fluorine was analyzed using TAP crystal instead of PC1 crystal of the X-ray spectrometer. Moreover, the FeO concentrations in our phonolitic glasses are low (<2 wt.%) and no overlapping between F and Fe peaks was observed using the analytical conditions described above. Multiple measurements were made for each sample (10–15 analyses) to reduce possible analytical errors and to check for homogeneity. Composition of major elements in minerals were analyzed with 15 kV acceleration potential, 15 nA beam current, a focused electron beam, and peak counting times of 5–10 s. The Cl and F concentrations in biotite were analyzed with a 30 nA beam current for 30 s.

2.4. Mass balance calculations

The fluid phase composition added to the starting dry glass is different from that in the run products due to significant differences in the partitioning of H_2O, Cl, and F as well as Na and K between fluid and melt. With the experimental strategy used in this study, the exact composition of the fluid phase cannot be measured directly (small amounts of fluid were used to minimize the effect of incongruent dissolution of the silicate components in the fluid) and a mass balance calculation was the only possible method to determine the fluid phase composition.

At 1000 °C, the run products were composed of quenched glass only, while at 845–865 °C the amount of mineral phases (mostly biotite (Bi) and a few plagioclase (Pl) and clinopyroxene (Cpx) crystals) was about ~5–10 vol.%. The amount of Bi was visually estimated to be ~2 to ~7.5 vol.% (Table 3). The amounts of Pl and Cpx were less than ~3–5 vol.%. In mass balance calculations we took only the concentrations of H_2O, F and Cl incorporated in Bi into account. The concentrations of Cl and F in Bi reach values up to 0.24±0.05 wt.% Cl and 0.95±0.05 wt.% F and are reported by Chevychelov et al. (2008a). The concentration of water was calculated from the structural formulae. In any case, the minor amount of Bi in the run products does not influence significantly the mass balance calculations.

The water content of the quenched glasses was estimated using various methods. The H_2O concentration in two nearly crystal-free samples (PG-45 and PG-48) was measured by Karl-Fischer titration (KFT; Behrens, 1995). It must be noted that the experimental glasses contained bubbles probably formed during quench. However, the KFT analysis is a bulk method and 5 to 10 mg of the glass was used for the measurements. Thus, the presence of tiny quench bubbles did not influence the quality of the data on bulk concentration of dissolved H_2O. The water contents of the glasses, determined by Karl-Fischer titration, were 5.8±0.1 and 5.2±0.1 wt.% for PG-45 and PG-48, respectively (Table 3). Another technique used for the determination of water concentration in the glasses was "by-difference method" (e.g., Devine et al., 1995; Freise et al., 2003). In this case, the difference from 100% of the electron microprobe total was calibrated using the

Table 3
Composition of phonolitic glass (wt.%±1σ) and mineral assemblages after experiments

Run number	n[a]	SiO_2	TiO_2	Al_2O_3	FeO_{tot}	MnO	MgO	CaO	Na_2O	K_2O	Cl	F	Total	H_2O[b]	H_2O[c]	A/CNK[d]	Mineral phases[e]
T=845–865 °C, P=200 MPa, f_{O2}=NNO																	
PG-13	14	56.2±0.4	0.16±0.03	19.7±0.2	1.7±0.3	0.2±0.1	0.15±0.06	2.3±0.2	4.9±0.4	9.0±0.2	–	–	94.3±0.8	5.25±0.7	6.4	0.90	Bi (?)
PG-61[f]	15	56.8±0.4	–	19.8±0.4	1.8±0.2	–	0.18±0.05	2.6±0.1	5.2±0.3	9.2±0.3	–	–	95.6±0.6	5.25±0.7	5.0	0.85	Cpx
PG-56[g]	14	56.8±0.6	0.18±0.03	19.8±0.3	1.3±0.1	0.1±0.1	0.19±0.05	2.7±0.1	5.2±0.4	9.0±0.3	0.29±0.01	–	95.6±0.7	5.45[i]±0.7	5.0	0.85	Bi (?), Cpx
PG-55[g]	15	57.0±0.8	0.17±0.04	19.6±0.4	1.3±0.2	0.1±0.1	0.19±0.03	2.5±0.1	4.8±0.3	8.9±0.3	0.50±0.02	–	95.1±0.7	4.9[i]±0.9	5.6	0.89	Bi (?), Pl
PG-54[g]	12	58.4±0.5	0.17±0.04	19.6±0.3	1.2±0.2	0.1±0.1	0.24±0.04	1.8±0.1	4.9±0.6	8.4±0.4	0.52±0.04	–	95.3±0.5	4.1[i]±1.7	5.3	0.96	Bi (?), Pl
PG-49	15	56.1±0.6	0.18±0.03	19.5±0.3	1.7±0.3	0.1±0.1	0.16±0.06	2.7±0.1	5.1±0.2	9.2±0.2	–	0.09±0.04	94.9±0.7	5.25±0.7	5.7	0.84	Bi (3)
PG-28	15	55.9±0.7	0.16±0.05	19.6±0.2	1.7±0.3	0.2±0.1	0.16±0.06	2.5±0.2	4.8±0.3	8.9±0.3	–	0.30±0.05	94.3±0.9	5.3±0.7	6.5	0.89	Bi (3)
PG-45	15	55.4±0.5	0.17±0.04	19.8±0.3	1.9±0.2	0.1±0.1	0.19±0.05	2.8±0.1	5.0±0.4	9.1±0.3	–	0.32±0.04	94.8±0.9	5.8[i]±0.1	5.9	0.85	Bi (3.5)
PG-27	12	56.0±0.6	0.18±0.04	19.3±0.4	1.6±0.3	0.1±0.1	0.16±0.05	2.5±0.3	4.7±0.3	9.0±0.2	–	0.73±0.14	94.3±0.9	5.6[i]±0.7	6.5	0.88	Bi (5)
PG-53	15	56.1±0.5	0.16±0.02	19.5±0.4	1.9±0.2	0.1±0.1	0.19±0.06	2.8±0.1	5.0±0.4	9.1±0.3	–	0.64±0.09	95.4±0.7	5.15[i]±0.7	5.2	0.84	Bi (2)
PG-48	15	56.1±0.3	0.15±0.04	19.7±0.2	1.8±0.3	0.2±0.1	0.19±0.04	2.8±0.1	4.9±0.5	9.1±0.2	0.30±0.01	0.10±0.03	95.4±0.7	5.2[i]±0.1	5.2	0.86	Bi (2.5)
PG-60[f]	15	56.5±0.6	–	19.7±0.4	1.8±0.2	–	0.20±0.07	2.8±0.1	5.1±0.3	9.1±0.2	0.29±0.01	0.31±0.03	95.8±1.0	5.3±0.7	4.7	0.84	Pl (?)
PG-25	14	55.8±0.4	0.19±0.04	19.6±0.7	1.4±0.3	0.1±0.1	0.16±0.04	2.5±0.2	4.6±0.5	8.9±0.3	0.20±0.01	0.48±0.04	94.0±1.0	5.3±0.7	6.8	0.90	Bi (5)
PG-12	8	55.3±0.5	0.19±0.03	19.6±0.3	1.8±0.2	0.1±0.1	0.19±0.05	2.5±0.4	4.9±0.4	8.9±0.2	0.37±0.01	0.56±0.23	94.4±0.7	5.35±0.7	6.3	0.88	Bi (5.5)
PG-16	15	55.2±0.6	0.18±0.04	19.7±0.3	1.5±0.2	0.1±0.1	0.15±0.04	2.6±0.2	4.9±0.2	8.8±0.3	0.31±0.01	0.54±0.06	94.0±0.9	4.25[i]±1.5	6.8	0.88	Bi (6.5)
PG-39	14	55.8±1.0	0.16±0.06	19.1±0.5	1.7±0.2	0.1±0.1	0.10±0.04	2.7±0.3	4.9±0.3	8.8±0.3	0.36±0.01	0.87±0.18	94.6±1.2	5.5±0.7	6.1	0.85	Bi (7.5)
PG-46	16	56.8±0.9	0.16±0.04	19.4±0.6	1.9±0.3	0.2±0.1	0.14±0.04	2.6±0.3	4.9±0.4	8.8±0.2	0.50±0.02	0.11±0.05	95.3±0.7	4.6[i]±1.2	5.3	0.87	Bi (6)
PG-59[f, g]	17	56.8±0.6	–	19.9±0.5	1.3±0.3	–	0.22±0.07	2.7±0.1	5.0±0.3	8.8±0.3	0.48±0.02	0.32±0.05	95.6±0.8	5.25±0.7	5.0	0.88	Pl, Cpx (?)
PG-11	16	55.9±0.5	0.17±0.04	19.3±0.3	1.5±0.2	0.2±0.1	0.13±0.06	2.6±0.3	4.4±0.4	8.3±0.2	0.58±0.04	0.66±0.11	93.8±0.9	5.35±0.7	7.1	0.92	Bi (5.5)
PG-52	15	56.0±0.7	0.15±0.05	19.4±0.5	1.8±0.3	0.1±0.1	0.17±0.05	2.8±0.2	4.8±0.3	8.8±0.2	0.60±0.04	0.62±0.06	95.3±0.9	5.15±0.7	5.3	0.86	Bi (3)
PG-9	16	55.4±0.5	0.16±0.03	19.8±0.3	1.7±0.3	0.2±0.1	0.13±0.04	2.6±0.2	4.9±0.4	8.7±0.4	0.60±0.04	0.45±0.05	94.6±0.8	5.2±0.7	6.1	0.89	Bi (7)
PG-8	12	56.2±0.5	0.17±0.04	19.5±0.3	1.5±0.2	0.1±0.1	0.17±0.06	2.7±0.2	4.5±0.4	8.0±0.3	0.62±0.05	0.56±0.05	94.1±0.9	5.2±0.7	6.7	0.93	Bi (5), Pl
PG-58[f, g]	14	58.9±0.6	–	19.6±0.3	1.1±0.2	–	0.23±0.06	1.7±0.1	4.7±0.3	8.5±0.3	0.48±0.02	0.11±0.03	95.5±0.8	5.0±0.8	5.1	0.98	Pl
PG-41	13	58.9±1.6	0.12±0.06	18.5±0.7	1.5±0.2	0.1±0.1	0.07±0.03	1.8±0.2	4.7±0.5	8.3±0.6	0.48±0.03	0.15±0.04	94.6±1.3	5.0±0.8	6.2	0.93	Bi (7)
PG-40	12	57.5±0.8	0.18±0.03	19.1±0.5	1.4±0.2	0.1±0.1	0.12±0.06	2.1±0.2	4.9±0.3	7.5±0.6	0.55±0.04	0.45±0.06	93.9±1.6	4.9±0.9	6.9	0.96	Bi (6)
PG-51	15	56.9±0.6	0.13±0.05	19.4±0.3	1.5±0.2	0.1±0.1	0.11±0.06	2.7±0.1	4.6±0.3	8.4±0.2	0.72±0.07	0.68±0.10	95.4±0.6	4.55±1.2	5.2	0.90	Bi (4.5)
T=1000 °C, P=200 MPa, f_{O2}=~NNO+3.5																	
PR-72[f, h]	4	53.2±0.5	–	19.9±0.3	1.5±0.4	–	0.26±0.11	2.3±0.2	5.1±0.2	9.3±0.2	–	–	91.6±0.5	6.0[i]±0.4	–	0.88	–
PR-70[f, h]	7	53.9±0.6	–	20.2±0.3	1.5±0.3	–	0.31±0.12	2.3±0.1	5.2±0.2	9.3±0.2	0.35±0.03	–	93.1±0.9	6.0±0.8	–	0.88	–
PR-66[f, h]	10	54.0±0.6	–	20.3±0.4	1.4±0.4	–	0.36±0.10	2.3±0.2	4.9±0.2	9.1±0.3	0.52±0.04	–	92.9±0.9	6.0[i]±0.8	–	0.92	–
PR-60[f, h]	11	55.5±0.6	–	20.6±0.3	0.7±0.3	–	0.26±0.07	2.2±0.2	4.4±0.2	8.3±0.3	0.61±0.06	–	92.5±0.9	6.0[i]±0.8	–	1.03	–

PR-71[f, h]	7	53.3±0.6	–	19.9±0.3	1.7±0.3	–	0.29±0.11	2.2±0.2	5.3±0.2	9.5±0.2	–	0.24±0.05	92.3±0.8	6.0±0.8	–	0.87	–
PR-68[f, h]	10	53.6±0.6	–	19.9±0.3	1.6±0.3	–	0.26±0.07	2.3±0.2	5.1±0.3	9.7±0.3	–	0.51±0.08	92.9±0.7	6.0±0.8	–	0.87	–
PR-63[f, h]	10	53.3±0.5	–	20.1±0.3	1.1±0.2	–	0.24±0.07	2.3±0.3	5.2±0.3	9.5±0.4	–	1.35±0.23	93.0±1.2	6.0±0.8	–	0.88	–
PR-69[f, h]	9	53.8±0.5	–	20.0±0.3	1.5±0.2	–	0.26±0.08	2.3±0.2	5.1±0.2	9.5±0.3	0.39±0.04	0.20±0.06	92.9±0.9	6.0±0.8	–	0.88	–
PR-67[f, h]	10	53.8±0.5	–	19.9±0.2	1.6±0.3	–	0.25±0.08	2.3±0.2	5.0±0.2	9.6±0.3	0.36±0.03	0.51±0.06	93.2±0.8	6.0±0.8	–	0.87	–
PR-62[f, h]	10	53.1±0.7	–	19.9±0.4	1.1±0.3	–	0.27±0.07	2.2±0.2	5.0±0.3	9.4±0.3	0.34±0.03	1.30±0.07	92.6±0.6	6.0[i]±0.8	–	0.88	–
PR-65[f, h]	10	53.6±0.6	–	20.0±0.3	1.5±0.3	–	0.23±0.08	2.2±0.2	4.8±0.2	9.1±0.3	0.53±0.04	0.20±0.04	92.0±0.4	6.0±0.8	–	0.92	–
PR-64[f, h]	11	54.0±0.5	–	19.9±0.3	1.2±0.3	–	0.24±0.06	2.2±0.2	4.8±0.3	9.0±0.4	0.54±0.04	0.59±0.10	92.4±0.8	6.0±0.8	–	0.93	–
PR-61[f, h]	10	53.6±0.7	–	20.0±0.3	0.8±0.3	–	0.26±0.11	2.2±0.1	4.8±0.2	9.0±0.3	0.67±0.05	1.31±0.10	92.5±0.6	6.0[i]±0.8	–	0.92	–
PR-59[f, h]	11	55.4±0.5	–	20.6±0.3	1.1±0.3	–	0.23±0.06	2.1±0.2	4.5±0.3	8.2±0.3	0.67±0.04	0.21±0.06	92.9±1.1	5.8±0.9	–	1.02	–
PR-58[f, h]	11	55.4±0.5	–	20.4±0.3	0.6±0.4	–	0.26±0.11	2.1±0.2	4.5±0.2	8.5±0.3	0.69±0.05	0.49±0.08	92.8±1.1	5.6±0.9	–	1.00	–
PR-57[f, h]	11	54.1±0.6	–	20.2±0.3	0.7±0.2	–	0.24±0.05	2.2±0.2	4.5±0.3	8.6±0.4	0.78±0.06	1.04±0.07	92.2±0.7	5.4[i]±1.0	–	0.98	–
PG-72[f]	10	57.1±0.5	–	19.7±0.3	2.0±0.4	–	0.19±0.06	2.5±0.2	4.7±0.4	8.5±0.2	–	–	94.7±0.5	6.1[i]±0.4	6.0	0.92	–
PG-77[f]	10	56.5±0.5	–	19.7±0.4	2.0±0.2	–	0.20±0.05	2.6±0.2	4.8±0.4	8.3±0.1	0.36±0.01	–	94.5±0.9	6.05±0.8	6.3	0.91	–
PG-73[f]	10	57.4±0.6	–	19.6±0.3	1.5±0.3	–	0.06±0.05	2.8±0.2	4.3±0.2	7.7±0.2	0.44±0.08	–	94.0±0.9	5.95[i]±0.8	6.9	0.96	–
PG-78[f]	10	56.5±0.4	–	19.6±0.3	2.1±0.4	–	0.24±0.06	2.6±0.2	5.1±0.4	8.7±0.2	–	0.11±0.03	95.0±0.8	6.15±0.8	5.7	0.87	–
PG-80[f]	10	56.4±0.6	–	19.3±0.3	2.0±0.3	–	0.20±0.09	2.6±0.2	4.7±0.3	8.7±0.3	–	0.36±0.06	94.4±0.7	6.25±0.8	6.4	0.88	–
PG-67[f]	6	56.2±0.4	–	19.7±0.1	2.1±0.3	–	0.21±0.08	1.9±0.3	4.8±0.7	8.7±0.2	–	0.32±0.05	94.1±1.2	6.45±0.9	6.8	0.95	–
PG-79[f]	10	56.6±0.7	–	19.5±0.3	2.1±0.3	–	0.17±0.04	2.7±0.3	5.1±0.3	8.5±0.2	0.36±0.01	0.13±0.03	95.1±0.9	6.1±0.8	5.6	0.87	–
PG-81[f]	10	56.0±0.5	–	19.3±0.3	2.0±0.2	–	0.17±0.04	2.7±0.1	4.9±0.5	8.5±0.3	0.37±0.02	0.37±0.03	94.3±0.8	6.15±0.8	6.5	0.87	–
PG-75[f]	10	57.0±0.7	–	20.3±0.4	1.7±0.3	–	0.12±0.06	1.9±0.6	4.5±0.2	7.9±0.2	0.36±0.01	0.30±0.11	94.2±0.6	6.4[i]±0.8	6.7	1.05	–
PG-82[f]	10	56.7±0.6	–	19.7±0.2	1.6±0.3	–	0.11±0.06	2.9±0.2	4.6±0.2	7.9±0.3	0.50±0.06	0.11±0.04	94.1±0.4	6.05±0.8	6.7	0.92	–
PG-74[f]	10	57.1±0.5	–	19.7±0.3	1.4±0.3	–	0.05±0.04	2.9±0.2	4.6±0.3	7.7±0.3	0.54±0.04	0.34±0.07	94.3±0.8	6.1±0.8	6.5	0.93	–
PG-68[f]	10	56.9±0.4	–	19.6±0.3	1.5±0.3	–	0.08±0.05	2.1±0.2	4.7±0.3	8.2±0.3	0.64±0.05	0.41±0.06	94.0±0.6	6.35[i]±0.8	6.8	0.96	–
PG-70[f]	10	57.6±0.5	–	19.8±0.3	1.8±0.4	–	0.17±0.06	2.5±0.2	4.6±0.3	7.8±0.2	0.70±0.04	0.30±0.03	95.3±1.1	5.7±0.9	5.4	0.96	–
PG-71[f]	10	56.9±0.6	–	19.6±0.3	1.7±0.2	–	0.13±0.02	2.6±0.2	4.5±0.3	8.1±0.2	0.82±0.04	0.44±0.05	94.9±0.7	5.0[i]±1.4	5.8	0.94	–

[a]Number of electron microprobe analyses.
[b,j,i]Water content of the melt (wt.%) estimated using ([j]) the Karl-Fischer titration method, ([i]) the "water mass balance method", and the interpolation and analogy for other runs (see 2.4. Mass balance calculations).
[c]Water content of the melt (wt.%) estimated using the "by-difference method" (see Mass balance calculations in the text).
[d]Molar $Al_2O_3/(CaO+Na_2O+K_2O)$ ratio of experimental glasses.
[e]Mineral phases (vol.%), determined by visual assessment and microprobe analysis in experimental products. (?) — content of this phase is not certain.
[f]All the experiments were done with starting material — "A" (Table 1) except those marked with ([f]) done with starting material — "B".
[g,h]All the experiments were done in Au capsules except those marked with ([g]) done in $Au_{80}Pd_{20}$ capsules, and with ([h]) done in Pt capsules.

quenched glasses with known H_2O contents (measured by KFT) from PG-45 and PG-48 experiments. To minimize the influence of quench bubbles on the results of the "by-difference method", we used the defocused (10–20 μm or 50×50 μm) electron beam for glass analysis and chose places on the sample with minimum amount of quench bubbles. The estimated uncertainty of this method is < 1.0 wt.% H_2O. In addition, the water contents of the quenched glasses from most experiments (see Table 3 for detail) were estimated using "water mass balance method", i.e., they were calculated as follows:

$$C^{gl}_{H_2O} = C^{fl,st}_{H_2O} \times ((M^{fl,st} - M^{fl,ev})/(M^{sil,st} + M^{fl,st} - M^{fl,ev})), \quad (1)$$

where $C^{fl,st}_{H_2O}$ is concentration of H_2O (wt.%) in starting solution, $(M^{fl,st} - M^{fl,ev})/(M^{sil,st} + M^{fl,st} - M^{fl,ev})$ is the weight fraction of the fluid dissolved

Table 4
The Cl, F, H_2O contents (wt.%) in the aqueous fluid determined by the mass balance calculation, and relationship between Cl and F among phases during the experiments (±1σ)

Run number	Cl in fluid	F in fluid	H_2O in fluid	Cl/F in fluid[a]	Cl/F in melt [a]	$^{fl/m}D_{Cl}$ [b] fluid/melt	$^{fl/m}D_F$ [b] fluid/melt	$^{fl/m}K_{D\ Cl/F}$ [b]	Fluid/melt in the run[c]
T=845–865 °C, P=200 MPa, f_{O2}=NNO									
PG-13	0	0	100	–	–	–	–	–	0.10
PG-61[d]	0	0	100	–	–	–	–	–	0.11
PG-56[e]	2.3 (0.4)	0	97.7 (0.4)	–	–	7.8 (1.6)	–	–	0.045
PG-55[e]	13.7 (3.5)	0	86.3 (3.5)	–	–	27.4 (6.9)	–	–	0.045
PG-54[e]	35.5 (14.5)	0	64.5 (14.5)	–	–	68.2 (28.4)	–	–	0.05
PG-49	0	2.1 (1.2)	97.9 (1.2)	0	0	–	23.4 (15.9)	–	0.04
PG-28	0	3.5 (0.7)	96.5 (0.7)	0	0	–	11.8 (3.0)	–	0.08
PG-45	0	6.0 (0.9)	94.0 (0.9)	0	0	–	18.4 (3.9)	–	0.045
PG-27	0	8.3 (2.0)	91.7 (2.0)	0	0	–	11.4 (3.5)	–	0.07
PG-53	0	15.0 (2.6)	85.0 (2.6)	0	0	–	23.4 (5.2)	–	0.035
PG-48	1.9 (0.8)	2.0 (0.7)	96.1 (0.9)	0.9 (0.6)	3.0 (0.5)	6.3 (2.2)	20.2 (9.6)	0.3 (0.2)	0.045
PG-60[d]	1.0 (0.1)	2.9 (0.4)	96.1 (0.4)	0.3 (0.07)	0.9 (0.1)	3.5 (0.6)	9.3 (1.6)	0.4 (0.1)	0.09
PG-25	2.0 (0.2)	3.9 (0.5)	94.1 (0.5)	0.5 (0.1)	0.4 (0.04)	10.2 (1.3)	8.0 (1.3)	1.3 (0.3)	0.09
PG-12	0.5 (0.2)	5.6 (2.8)	93.8 (2.8)	0.09 (0.08)	0.7 (0.3)	1.4 (0.7)	10.1 (6.5)	0.14 (0.1)	0.07
PG-16	1.1 (0.2)	6.6 (1.3)	92.3 (1.3)	0.16 (0.03)	0.6 (0.07)	3.5 (0.7)	12.3 (2.7)	0.3 (0.1)	0.08
PG-39	2.4 (0.6)	11.9 (2.9)	85.7 (3.0)	0.2 (0.08)	0.4 (0.09)	6.9 (1.6)	13.6 (4.4)	0.5 (0.2)	0.06
PG-46	12.8 (8.8)	1.7 (1.2)	85.5 (9.1)	7.6 (7.4)	4.5 (1.7)	25.6 (17.7)	15.4 (12.5)	1.7 (1.8)	0.06
PG-59[d, e]	7.0 (1.7)	2.9 (0.7)	90.2 (1.9)	2.4 (0.7)	1.5 (0.2)	14.5 (3.5)	9.0 (2.5)	1.6 (0.6)	0.11
PG-11	7.9 (1.9)	6.6 (1.5)	85.5 (2.4)	1.2 (0.4)	0.9 (0.2)	13.6 (3.1)	10.1 (2.8)	1.4 (0.5)	0.09
PG-52	14.4 (2.0)	18.2 (2.6)	67.4 (3.2)	0.8 (0.2)	1.0 (0.1)	24.0 (3.9)	29.3 (5.1)	0.8 (0.2)	0.035
PG-9	17.8 (2.9)	3.1 (0.5)	79.2 (3.0)	5.8 (1.3)	1.3 (0.2)	29.6 (5.1)	6.8 (1.2)	4.4 (1.1)	0.10
PG-8	20.0 (2.7)	10.0 (1.3)	70.0 (3.0)	2.0 (0.4)	1.1 (0.1)	32.2 (5.1)	17.8 (2.9)	1.8 (0.4)	0.10
PG-58[d, e]	25.8 (10.5)	1.3 (0.5)	72.9 (10.6)	20.2 (11.8)	4.4 (1.2)	53.7 (22.1)	11.6 (5.6)	4.6 (3.0)	0.09
PG-41	38.4 (15.0)	1.0 (0.4)	60.6 (15.1)	38.8 (22.1)	3.2 (0.9)	80.1 (32.0)	6.6 (3.2)	12.1 (7.6)	0.06
PG-40	35.6 (7.1)	4.5 (0.9)	59.9 (7.3)	8.0 (2.2)	1.2 (0.2)	64.7 (13.8)	9.9 (2.5)	6.5 (2.2)	0.07
PG-51	39.0 (9.3)	13.3 (3.1)	47.7 (10.1)	2.9 (0.9)	1.1 (0.2)	54.2 (13.9)	19.6 (5.5)	2.8 (1.1)	0.05
T=1000 °C, P=200 MPa, f_{O2}=~NNO+3.5									
PR-72[d, f]	0	0	100	–	–	–	–	–	0.07
PR-70[d, f]	1.8 (0.5)	0	98.2 (0.5)	–	–	5.1 (1.3)	–	–	0.06
PR-66[d, f]	13.6 (3.5)	0	86.4 (3.5)	–	–	26.1 (8.3)	–	–	0.07
PR-60[d, f]	36.3 (9.4)	0	63.7 (9.4)	–	–	59.5 (19.1)	–	–	0.07
PR-71[d, f]	0	0.33 (0.13)	99.7 (0.1)	0	0	–	1.4 (0.6)	–	0.07
PR-68[d, f]	0	3.1 (0.8)	96.9 (0.8)	0	0	–	6.1 (1.8)	–	0.06
PR-63[d, f]	0	5.9 (1.4)	94.1 (1.4)	0	0	–	4.4 (1.3)	–	0.06
PR-69[d, f]	1.5 (0.4)	0.6 (0.2)	97.9 (0.4)	2.4 (1.1)	1.9 (0.5)	3.8 (1.3)	3.1 (1.2)	1.2 (0.6)	0.07
PR-67[d, f]	1.9 (0.2)	3.2 (0.4)	94.9 (0.4)	0.6 (0.1)	0.7 (0.07)	5.2 (0.8)	6.3 (1.0)	0.8 (0.2)	0.06
PR-62[d, f]	2.6 (1.1)	6.4 (2.6)	91.0 (2.8)	0.4 (0.2)	0.26 (0.1)	7.6 (3.2)	4.9 (2.2)	1.5 (0.8)	0.055
PR-65[d, f]	13.8 (7.1)	0.6 (0.3)	85.6 (7.1)	23.3 (17.1)	2.6 (1.0)	26.0 (13.8)	2.9 (1.7)	8.9 (6.8)	0.07
PR-64[d, f]	14.4 (4.3)	2.3 (0.7)	83.2 (4.5)	6.2 (2.4)	0.9 (0.2)	26.8 (7.9)	4.0 (1.4)	6.7 (3.0)	0.07
PR-61[d, f]	14.0 (3.0)	6.4 (1.3)	79.6 (3.3)	2.2 (1.2)	0.5 (0.1)	21.0 (4.7)	4.9 (1.2)	4.3 (1.4)	0.06
PR-59[d, f]	35.0 (5.2)	0.5 (0.1)	64.5 (5.2)	63.7 (13.2)	3.3 (0.4)	52.2 (8.4)	2.7 (0.5)	19.5 (4.9)	0.07
PR-58[d, f]	35.7 (5.3)	2.4 (0.4)	61.9 (5.4)	14.8 (3.1)	1.4 (0.16)	51.7 (8.3)	4.9 (0.9)	10.5 (2.6)	0.07
PR-57[d, f]	38.0 (7.3)	6.2 (1.2)	55.8 (7.6)	6.2 (2.8)	0.75 (0.1)	48.7 (9.7)	6.0 (1.3)	8.2 (2.2)	0.06
PG-72[d]	0	0	100	–	–	–	–	–	0.03
PG-77[d]	1.3 (0.4)	0	98.7 (0.4)	–	–	3.7 (0.9)	–	–	0.05
PG-73[d]	15.9 (4.2)	0	84.1 (4.2)	–	–	36.2 (11.7)	–	–	0.05
PG-78[d]	0	2.1 (0.9)	97.9 (0.9)	0	0	–	19.4 (9.2)	–	0.04
PG-80[d]	0	5.9 (1.5)	94.1 (1.5)	0	0	–	16.4 (4.7)	–	0.045
PG-67[d]	0	30.9 (6.9)	69.1 (6.9)	0	0	–	96.5 (26.5)	–	0.03
PG-79[d]	1.3 (0.4)	1.8 (0.6)	96.8 (0.7)	0.7 (0.4)	2.8 (0.7)	3.6 (1.3)	14.2 (5.9)	0.3 (0.1)	0.045
PG-81[d]	0.5 (0.05)	6.2 (0.7)	93.3 (0.7)	0.08 (0.02)	1.0 (0.1)	1.3 (0.2)	16.7 (2.6)	0.08 (0.02)	0.035
PG-75[d]	0.06 (0.04)	36.6 (19.4)	63.3 (19.4)	0.002	1.2 (0.4)	0.18 (0.09)	122 (79)	0.001	0.025
PG-82[d]	16.5 (8.6)	2.4 (1.2)	81.1 (8.8)	7.0 (5.2)	4.5 (1.7)	33.1 (18.0)	21.6 (13.8)	1.5 (1.2)	0.04
PG-74[d]	15.9 (4.7)	6.8 (2.0)	77.3 (5.3)	2.4 (0.9)	1.6 (0.4)	29.5 (9.0)	19.9 (7.3)	1.5 (0.7)	0.045
PG-68[d]	20.0 (4.3)	40.4 (8.5)	39.6 (9.5)	0.5 (1.3)	1.6 (0.3)	31.3 (7.0)	98.5 (25.3)	0.3 (0.1)	0.02
PG-70[d]	53.3 (7.9)	9.7 (1.5)	37.0 (8.3)	5.5 (1.1)	2.3 (0.3)	76.1 (12.1)	32.4 (5.8)	2.3 (0.6)	0.03
PG-71[d]	65.5 (12.6)	33.2 (6.4)	1.3 (14)	2.0 (0.9)	1.9 (0.2)	79.8 (16.0)	75.5 (16.9)	1.1 (0.3)	0.02

[a] (C_{Cl} in fluid (in melt), wt.%)/(C_F in fluid (in melt), wt.%).
[b] Partition coefficients of Cl (F) between fluid and phonolitic melt — $^{fl/m}D_{Cl} = {}^{fl}C_{Cl}$ (wt.%)/$^{m}C_{Cl}$ (wt.%), and $^{fl/m}D_F = {}^{fl}C_F$ (wt.%)/$^{m}C_F$ (wt.%). Exchange coefficients of Cl/F between fluid and phonolitic melt — $^{fl/m}K_{D\ Cl/F} = {}^{fl/m}D_{Cl}/{}^{fl/m}D_F$.
[c] Fluid/melt ratio by weight calculated for run products.
[d] All the experiments were done with starting material — "A" (Table 1) except those marked with ([d]) done with starting material — "B".
[e,f] All the experiments were done in Au capsules except those marked with ([e]) done in $Au_{80}Pd_{20}$ capsules, and with ([f]) done in Pt capsules.

in the quenched glass, with *C* = concentration, wt.%; *M* = mass, mg; gl = glass in the run product; fl = fluid (solution); st = starting; ev = evaporated solution after 3 min at 110 °C; sil = phonolitic powder before the run. The errors of this "water mass balance method" are relatively large due to (1) the assumption that the fluid evaporated after opening of the capsule was composed of water only; (2) the possible incongruent dissolution of phonolitic glass into the fluid during the experiment which was not considered, and (3) the possible formation of water-bearing quench phases. However, in most cases, the water contents obtained using the "water mass balance method" were identical within uncertainty to those obtained by the "by-difference method" (Table 3).

Such a calculation for the PR-72 and PG-72 runs (at 1000 °C) allows us to estimate the water content in the quenched glass with a relatively small uncertainty of ±0.4 wt.% because pure H_2O was used as a starting solution and run products are composed of glass and fluid phase only. The water concentrations in glasses range from 4.1 to 5.8 wt.% ("water mass balance method"), and from 4.7 to 7.1 wt.% ("by-difference method") at 845–865 °C and from 5.0 to 6.5 wt.% ("water mass balance method") and from 5.4 to 6.9 wt.% ("by-difference method") at 1000 °C. These values are in a good agreement with the data of Iacono Marziano et al. (2007) and Schmidt and Behrens (2008-this issue) for K-rich phonolitic melt of Mt. Vesuvius. However, the data are lower than the water solubility values at 200 MPa for Na-phonolites [6.6 wt.% H_2O at 840 °C (Freise et al., 2003) and 8.4 wt.% H_2O at 850 °C (Larsen and Gardner, 2004) as well as 8.1 wt.% H_2O at 850 °C as extrapolated from low-pressure data of Carroll and Blank, 1997]. This difference may result from different bulk compositions, and especially from the different Na/K and Al/(Na+K) ratios. Considering that H_2O is preferentially associated to Na in silicate melts (Holtz et al., 1995), the observed difference is consistent with previous datasets.

The Cl and F concentrations in the bulk fluid were calculated using mass balance based on the initial amounts of Cl and F in the system and measured concentrations of Cl and F in the experimental products (Table 4). Chlorine and fluorine are partitioned among melt, fluid(s) and Bi at 845–865 °C and between melt and fluid(s) at 1000 °C. It must be noted, that measured concentrations of Cl and F in Cl- and F-rich systems are characterized by a relatively poor reproducibility and a large uncertainty in some samples (Table 3; Figs. 1 and 2) probably due to inhomogeneous distribution of volatiles in the melt or due to a presence of quench bubbles in glasses. This, in turn, increased the error of the mass balance calculations for the composition of the fluid phase(s). The concentrations of Cl and F in the fluid phase were calculated as bulk concentrations in the fluid, independently of the presence of one or two fluid phases during the experiment.

3. Results

3.1. Experimental products

The mineral assemblages and the compositions of the phonolitic glasses are summarized in Table 3. The analytical errors given in Table 3 correspond to one σ deviation of the analyses. The calculated ratios of the fluid to phonolitic melt after the run were in the range from 0.02 to 0.11 by weight (Table 4). Biotite was present as large crystals (the size of single crystals is up to 500–800 μm), concentrated near to the interface between silicate glass and capsule wall or close to the walls of the large vesicles. Bi was found only in the runs with the starting phonolitic glass "A" (see Table 1), implying that even low concentrations of Ti and Mn may stabilize Bi in phonolitic magmas. The $Mg^{\#}$ of Bi ($Mg^{\#}=100\times Mg/(Mg+Mn+Fe)$, molar ratio) is in the range from 41 to 57 (Chevychelov et al., 2008a). Pl and Cpx were homogeneously distributed within the samples as small crystals (the size ranges from few microns up to 50 μm).

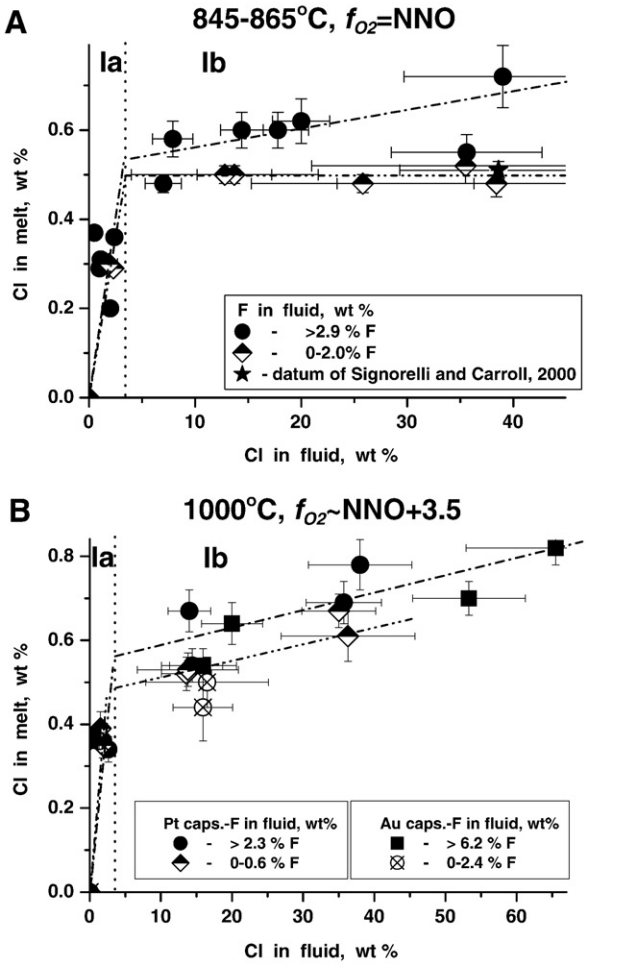

Fig. 1. The Cl content in phonolitic melt versus the Cl content in H_2O–Cl–F-bearing fluid (s) at 200 MPa, 845–865 °C, f_{O2} = NNO (A), and at 1000 °C, f_{O2} ~ NNO + 3.5 (B). Different symbols characterize samples from experiments in Pt and Au capsules as well as samples with different F concentrations in the fluid(s); the error bars are 1σ deviations. Dash–dotted line is interpretative line for F-rich system, and dash–double-dotted line is interpretative line for F-poor system. Star is after Signorelli and Carroll (2000) at 870 °C, 200 MPa, f_{O2} ~ NNO + 1, and F-free system. The vertical dotted line separates Ia field with Cl-poor fluid(s) and Ib field with Cl-rich fluid(s).

3.2. Major-element compositions of glasses

The major-element compositions of the glasses are listed in Table 3. At 845–865 °C, for systems rich in Cl and poor in F (runs of PG-58, PG-54, PG-41, PG-40), the experimental glasses contain less CaO (about 1.7–2.1 wt.%) than the starting composition. These compositions are also depleted in part in K_2O (7.5–8.5 wt.%), FeO (1.1–1.5 wt.%) and have higher A/CNK ratio (0.93–0.98). It implies that mineral crystallization or/and selective extraction of Ca, K and Fe from the melt by Cl-rich fluid affected the composition of the melt. All experiments conducted in Pt capsules at 1000 °C show systematically lower FeO concentrations (up to 70 rel.%, PR-58; Table 3) when compared with the starting composition, presumably due to loss of Fe into the capsule wall.

3.3. H_2O, Cl, and F contents of melt and aqueous fluid phases

The Cl, F, H_2O contents analyzed in the phonolitic glasses after the experiments are listed in Table 3. The concentrations of H_2O, Cl, and F in the aqueous fluid determined by the mass balance calculations are summarized in Table 4.

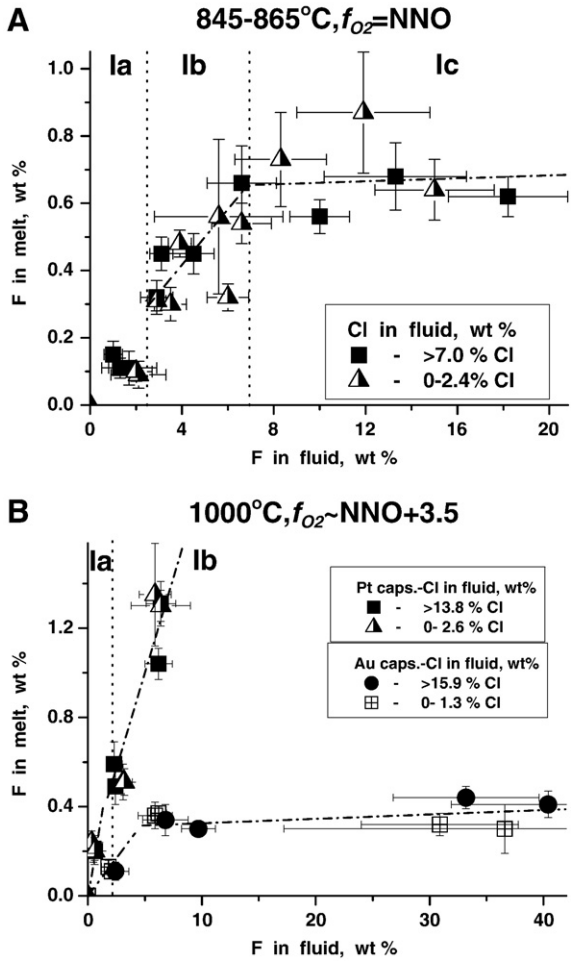

Fig. 2. The F content of phonolitic melt versus the F content in H_2O–Cl–F-bearing fluid(s) at 200 MPa, 845–865 °C, f_{O2}=NNO (A), and at 1000 °C, f_{O2}~NNO+3.5 (B). The symbols denote different Cl concentrations in the fluid(s) as well as runs in Pt and Au capsules in (B). Dash–dotted line is interpretative trend of the evolution of F content in the melt with increasing of F in the fluid(s). The vertical dotted lines in (A) separate Ia, Ib and Ic fields with F-poor, F-intermediate and F-rich fluid(s), respectively. The dotted line in (B) separates Ia and Ib fields with F-poor and F-rich fluid(s), respectively.

3.3.1. Solubilities of H_2O–Cl–F fluids in melt at 845–865 °C and NNO

Fig. 1A shows the Cl concentration in the melt (^{m}Cl) as a function of Cl content in the coexisting fluid (^{fl}Cl). With increasing ^{fl}Cl, the concentration of ^{m}Cl increases nonlinearly, i.e., there is a strong increase of ^{m}Cl with the first additions of Cl to the system (up to ~0.4 wt.% ^{m}Cl with ^{fl}Cl increase up to 2.4 wt.%; Ia field) but only minor increase of ^{m}Cl (from ~0.5 up to 0.7 wt.%; Ib area) with further increase of ^{fl}Cl up to ~39 wt.%. In the Ia field, Cl content in melt does not correlate within error with F concentration in the fluid phase (Fig. 1A). In the Ib field, at a given Cl concentration in the fluid, the ^{m}Cl shows systematically higher values in F-rich systems compared with F-poor and F-free systems. Moreover, the ^{m}Cl in F-rich systems continuously increases (from ~0.5 up to 0.7 wt.%, except sample PG-40 with ~36 wt.% ^{fl}Cl) while ^{m}Cl in F-poor systems remains almost constant (~0.5 wt.%) with ^{fl}Cl increase. The obtained results indicate that addition of F to the system may increase the concentration of Cl in the phonolitic melt by up to ~30 relative % at a given ^{fl}Cl. Our experimental data on the Cl concentration (^{m}Cl=0.52 wt.%) in synthetic phonolitic melt at 865 °C, f_{O2}=NNO, ^{fl}Cl=35.5 wt.%, F-poor system, fluid/melt ratio=0.05 (Fig. 1A) are in a good agreement with the results on Cl concentration (^{m}Cl=0.51 wt.%) obtained by Signorelli and Carroll (2000) at similar conditions (870 °C, 200 MPa, f_{O2}~NNO+1, initial 5 m (Na,K)Cl fluid, F-free Mt. Vesuvius phonolite, fluid/melt ratio=0.07).

The concentration of F in the melt (^{m}F) as a function of F content of the coexisting fluid (^{fl}F) is presented in Fig. 2A. At ^{fl}F contents lower than ~7 wt.%, ^{m}F increases from ~0.1 up to ~0.7 wt.% with increasing ^{fl}F (Ia and Ib fields in Fig. 2A). Despite the scattering of the data for ^{fl}F higher than ~7 wt.% (Ic field in Fig. 2A), the general trend indicates that ^{m}F is almost independent on ^{fl}F and remains approximately constant at 0.7±0.15 wt.% with increasing ^{fl}F up to ~18 wt.%. The effect of Cl on the partitioning of F between melt and fluid(s) at the studied conditions is not detectable.

3.3.2. Solubilities of H_2O–Cl–F fluids in melt at 1000 °C and ~NNO+3.5

Fig. 1B shows the ^{m}Cl as a function of Cl content in the equilibrium fluid(s). In both experimental series, i.e., in Au and Pt capsules, ^{m}Cl increases significantly up to ~0.4 wt.% with small additions of Cl to the system (^{fl}Cl<5 wt.%; Ia field in Fig. 1B). In contrast, small changes of ^{m}Cl are observed with further ^{fl}Cl increase (from ~0.4 up to 0.8 wt.% with increasing ^{fl}Cl up to 65 wt.%, Fig. 1B, Ib field). Although the obtained dataset does not provide a direct evidence for the effect of F on the Cl concentration in the melt at 1000 °C, data plotted in Fig. 1B indicate that in F-rich systems the ^{m}Cl at given ^{fl}Cl is generally higher than that in F-poor systems, in agreement with the experiments at 845–865 °C. The relationship between ^{m}Cl and ^{fl}Cl at 1000 °C is similar to that determined at 845–865 °C, indicating that variations of temperature in the range 850–1000 °C and of redox conditions in the range NNO–NNO+3.5 have no significant effect on the partitioning of Cl between fluid and phonolitic melt or, alternatively, that the effects of T and f_{O2} compensate each other.

Our experimental data (^{m}Cl=0.78 wt.%) at 1000 °C, ^{m}F=1.04 wt.%, ^{fl}Cl=38 wt.%, ^{fl}F=6.2 wt.% are close to the results on Cl concentration (^{m}Cl=0.80 wt.%) obtained by Webster and De Vivo (2002) at 1166 °C, 200 MPa for the Mt. Vesuvius phonolite (^{m}F=0.66 wt.%). It must be noted that the experiments of Webster and De Vivo (2002) were conducted in a Cl-rich system (NaCl+KCl added) with low H_2O concentration, indicating that the phonolitic melt was in equilibrium with a supercritical Cl-rich fluid phase at the studied conditions.

The evolution of ^{m}F as a function of ^{fl}F is presented in Fig. 2B. The results obtained in Au capsules indicate a non-linear dependence of ^{m}F on ^{fl}F, as observed for the runs in Au capsules at ~850 °C (Fig. 2A). In contrast, the results obtained in Pt capsules show that ^{m}F values increase almost linearly up to 1.4 wt.% with increasing ^{fl}F to 6–7 wt.%. This drastic discrepancy between the two datasets obtained at similar conditions and in the systems with similar bulk compositions but using Au and Pt capsules is surprising and indicative of a significant effect of capsule material on the behavior of F. Independently on the capsule material which has been used, the influence of Cl on the partitioning of F is not detectable within the uncertainty of the data.

4. Discussion

4.1. Experimental problems due to capsule material

The strong discrepancy between the experimental results on F partitioning between fluid and melt observed at 1000 °C indicates that at least one of the noble metals does not behave as an inert component in the presence of F. To our knowledge, previous experiments were not performed at similar conditions in both Au and Pt capsules and there is no available dataset in the literature illustrating the effect observed in Fig. 2B. The interpretation of the results obtained in Au capsule implies that an additional phase may buffer the F content in the melt at a given F content in the system. In addition, the F content in the glasses synthesized in Au capsules is systematically lower than that in glasses from Pt capsules. These observations indicate that in Au capsules, F is incorporated in an additional phase other than fluid and silicate melt. An additional phase (mineral or melt immiscibility) was not detected in the experimental products, and the most probable explanation is that F reacts with Au, forming complexes which

buffer the F activity in the experiments. Such a problem was not encountered with Cl, considering that the determined Cl concentrations in glasses and the calculated Cl concentration in the fluid are identical within uncertainty for the experiments conducted in both Au and Pt capsules.

Although this needs to be investigated in detail, the data obtained at high temperature with Au capsules will not be used in the following discussions. We expect that such Au–F-bearing complexes may not influence significantly the data at lower temperature. However, since most literature data on F distribution between fluid, melt and minerals at low temperature (<900 °C) have been obtained from experiments performed in Au capsules, the discrepancy observed in this study needs to be clarified.

4.2. Cl partitioning, Cl concentration in silicate melt and fluid immiscibility

The partition coefficients (D_{Cl}), expressed as the ratio of concentrations between coexisting fluid phase and melt are shown in Fig. 3 and listed in Table 4. Due to the fact that the complex H_2O–Cl–F-bearing fluid may have been composed of vapor and brine in the experiments with Cl-rich compositions, the results are presented as bulk partition coefficients of Cl between fluid(s) and melt ($^{fl/m}D = {}^{fl}C/{}^{m}C$) because only bulk concentrations of Cl in the fluid(s) could be determined. Even if some of the D_{Cl} values determined in this study are apparent (bulk) values (if two fluids coexist), the obtained data ranging from 1.4 to 80 (ratio in wt.%) are comparable with the data of other investigations (e.g., Signorelli and Carroll, 2000). In previous studies, $^{fl/m}D_{Cl}$ varied over a wide range from 5 to more than 100 for felsic melts (Kilinc and Burnham, 1972; Malinin et al., 1989; Shinohara et al., 1989; Webster, 1992a,b; Kravchuk and Keppler, 1994; Malinin and Kravchuk, 1995; Webster and Rebbert, 1998; Chevychelov, 1999) and were significantly lower for basaltic and andesitic melts, ranging from 0.3 to 6 in the available datasets (Gorbachev, Khodorevskaya, 1995; Webster et al., 1999; Mathez and Webster, 2005; Chevychelov et al., 2008b).

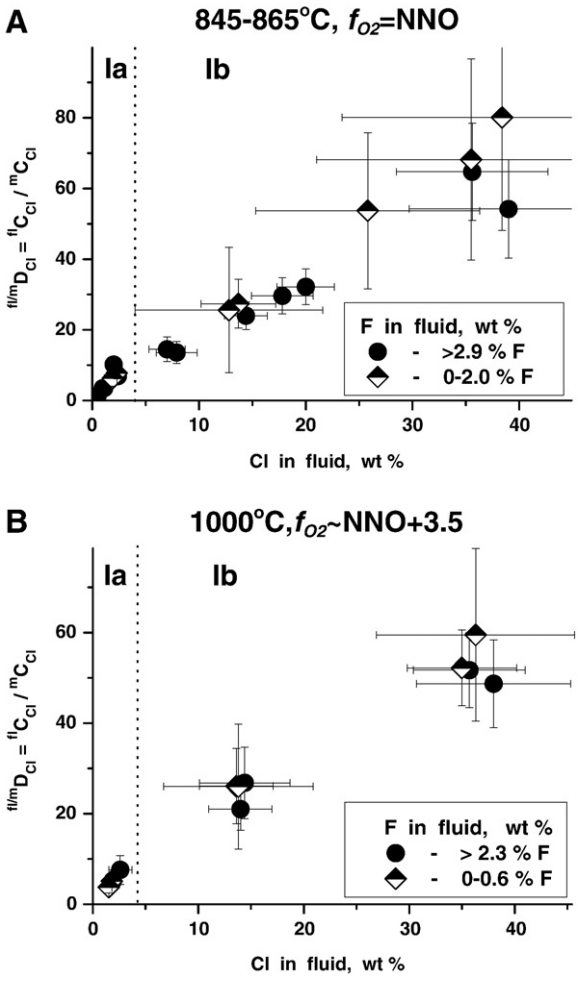

Fig. 3. The partition coefficients of Cl between fluid(s) and phonolitic melt ($^{fl/m}D_{Cl} = {}^{fl}C_{Cl}/{}^{m}C_{Cl}$, wt.% ratio) versus Cl contents in H_2O–Cl–F-fluid phase(s) at 845–865 °C (A) and 1000 °C (B). At 1000 °C (B), only experiments in Pt capsules are shown. Different symbols characterize samples with different F concentrations in the fluid(s). The vertical dotted line separates Ia and Ib fields with Cl-poor and Cl-rich fluid(s), respectively.

The observed non-linear relationships between ^{fl}Cl and ^{m}Cl (Fig. 1A and B) indicate that the behavior of volatile components in the melt–fluid(s) system was far from ideal at both studied temperatures. Fluid immiscibility (i.e., a H_2O-rich fluid coexisting with a Cl-rich brine) is not expected at our experimental *P–T* conditions (~850 °C, 200 MPa) for the H_2O–Cl-bearing system (according to the data for the H_2O–NaCl fluids reported by Chou, 1987; Anderko and Pitzer, 1993). However, at 845–865 °C, the observation of nearly constant ^{m}Cl values ~0.5 wt.% at ^{fl}Cl>5 wt.% for F-free or F-poor fluids (Fig. 1A) is an evidence for the presence of two fluids (brine and vapor; e.g., Shinohara et al., 1989). Fig. 1A shows that ^{m}Cl values may increase with increasing amount of F in the system and may reach up to ~0.7 wt.% in a melt, coexisting with a fluid containing high Cl (39 wt.%) and F (13.3 wt.%) concentrations (see also Table 4). Thus, the available dataset indicates either (1) that only one fluid exists at high ^{fl}F in a strongly non-ideal melt–fluid system or (2) that increasing F concentration in the system continuously reduces the immiscibility gap in H_2O–Cl-bearing fluid. Although it is difficult to decide whether one or two fluid phases are present at high ^{fl}F, the results indicate that the system was very close to critical conditions with strongly non-ideal behavior of H_2O- and Cl-bearing volatiles. The dataset at 1000 °C shows also a non-ideality of fluid mixing with probably similar effect of increasing F concentration in the system (Fig. 1B). The highest ^{m}Cl (0.78 wt.%) has been indeed determined in the sample with the highest ^{fl}F (6.2 wt.%; Fig. 1B, Table 4).

The data of Signorelli and Carroll (2000) obtained in the pressure range from 25 to 250 MPa show that the unmixing of the fluid phase coexisting with phonolitic melt should occur at pressures slightly below 200 MPa. Our experiments in F-free and F-poor systems indicate that two fluid phases may already be present at 200 MPa. This difference in the critical conditions can be caused by the differences in the initial fluid composition, i.e., (Na,K)Cl was added to the phonolite composition by Signorelli and Carroll (2000) and HCl was used in this work. Consequently, the composition of the equilibrium fluid(s) and the phase relationships could be slightly different in both studies.

4.3. F partitioning, F concentration in silicate melt and fluid immiscibility

The apparent partition coefficients (D_F) between fluid (bulk fluid) and melt are shown in Fig. 4 and listed in Table 4. In Fig. 4A, $^{fl/m}D_F$ values in the Ia field (F-poor fluid, see also Fig. 2A) have high relative uncertainties and the variations observed as a function of ^{fl}F are probably artifacts, resulting from the mass balance calculation (the bulk concentration of F in the fluid is very low). Hence, these data are not considered in the following discussion. According to our experimental results at 1000 °C (Pt capsules, Fig. 2B) and 845–865 °C, increasing temperature may cause a decrease of D_F in phonolitic melts.

Our experimental data indicate that at 845–865 °C immiscibility between a low and a high density fluid phase may occur in Cl-poor, F-rich phonolitic systems (Fig. 2A). Several experimental charges with small amounts or no Cl plot within the Ic field in Fig. 2A, indicating that ^{m}F is nearly constant with increasing ^{fl}F. Fluid immiscibility in the H_2O–F-bearing system has not been investigated in detail. Based on the available experimental data (Ravich and Valyashko, 1965; Urusova and Ravich, 1966; Ravich, 1974; Kotelnikova and Kotelnikov, 2002; Dolejs and

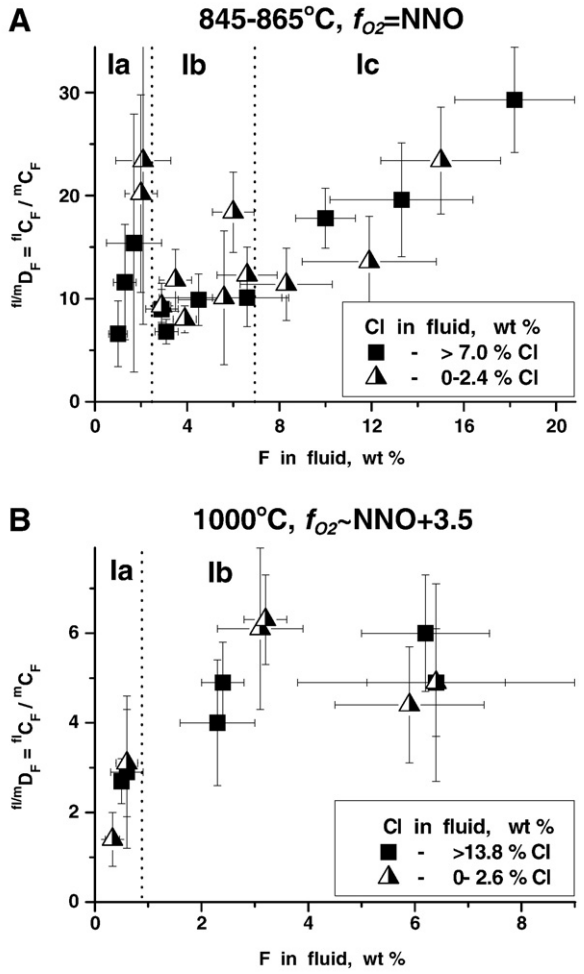

Fig. 4. The partition coefficients of F between fluid(s) and phonolitic melt ($^{fl/m}D_F = {}^{fl}C_F/{}^{m}C_F$, wt.% ratio) versus F contents in H_2O–Cl–F-fluid phase(s) at 845–865 °C (A) and 1000 °C (B). At 1000 °C (B), only experiments in Pt capsules are shown. The symbols denote different Cl concentrations in the fluid(s). The vertical dotted lines in (A) separate Ia, Ib and Ic fields with F-poor, F-intermediate and F-rich fluid(s), respectively. The dotted line in (B) separates Ia and Ib fields with F-poor and F-rich fluid(s), respectively.

Baker, 2007b), two fluids might be stable at our experimental *P–T* conditions (low-density aqueous vapor and hydrous fluoride melt). Experimental data on F concentration in melts of phonolitic composition saturated with respect to a F-bearing phase (e.g., fluorite, vapor, brine) are absent. Considering that no solid F-bearing phase is observed in our experimental products, the fluid phase(s) probably control the maximum F concentration of the phonolitic melt, due to the buffering of F activity by the formation of immiscible fluids at 845–865 °C. On the other hand, the experimental data at 845–865 °C need to be interpreted with caution (especially for high F content in the system) as long as the discrepancy between data obtained in Au and Pt capsules is not clarified.

Even if some of the $^{fl/m}D_F$ values shown in Fig. 4 may be interpreted with caution (especially from experiments in which two fluids may coexist), a general comparison between the dataset obtained for phonolitic and rhyolitic systems is possible. The $^{fl/m}D_F$ values obtained in our experiments are high and always >1 (wt.% ratio). This is surprising when compared with results obtained for silicic melts. It is generally assumed that fluorine is preferentially partitioned into aluminosilicate melts rather than in fluids and the partition coefficients of F between fluid and felsic melts are 0.1–0.5 at ^{fl}F less than 1 wt.% and up to 1.1 with increasing ^{fl}F up to 8.0 wt.% (Kovalenko, 1977; Webster, 1990; Webster and Holloway, 1990; Keppler and Wyllie, 1991; Chevychelov et al., 2005). The explanation for high $^{fl/m}D_F$ values could be related to the properties of phonolitic melts, to the use of HF solutions as a starting solution, and to the relatively high bulk F contents in the system. However, the high F contents in the system do not explain the high (>1) D_F values because most of the previous experiments have been conducted over a similar range of bulk F contents. Keppler and Wyllie (1991) observed that the use of initial HF solutions instead of NaF in experiments has a positive effect on the D_F values in haplogranitic systems, but the D_F were always found to be below 1. Thus, even if some high D_F values may be due to the use of HF, this cannot completely explain the D_F values above unity observed in this study. D_F values >1 have also been determined for a basaltic system (Chevychelov et al., in press-b), indicating that the partitioning of F between depolymerized melts and fluids may differ significantly from that in polymerized silicic melts.

4.4. Cl and F concentration in phonolitic melts and implications for Mt. Vesuvius

Mt. Somma–Vesuvius has erupted numerous Cl-bearing alkali-rich lavas and Cl-rich fluids during the past several thousand years. This composite volcano consists of the older Mt. Somma caldera, formed between 14 and 3.55 ka before present, and the younger Vesuvius cone. Magmatic activity has been well characterized through investigations of whole-rock samples and silicate melt inclusions (e.g., Santacroce et al., 1993; Marianelli et al., 1995; Belkin et al., 1998; Marianelli et al., 1999; Signorelli et al., 1999; Cioni, 2000; Raia et al., 2000; Webster et al., 2001; Webster and De Vivo, 2002; Lima et al., 2007). The data show distinct differences in composition for eruptive products older than 14 ka versus eruptive products younger than 3.55 ka. The older pre-caldera eruptions were associated with magmas relatively enriched in SiO_2, whereas eruptions younger than 3.55 ka were derived from magmas comparatively enriched in Cl, F, P_2O_5, S, and many lithophile trace elements (Webster et al., 2001). Studies on fluid inclusions in mafic nodules as well as structural features and geodynamics of the Mt. Somma–Vesuvius volcano suggest that crystallization processes might have taken place in a shallow magma chamber located approximately 4 to 7 km below surface that correspond to *P*~100–200 MPa (Cioni, 2000; Webster and De Vivo, 2002; De Natale et al., 2006; Lima et al., 2007). Clinopyroxene- and olivine-hosted melt inclusions yield homogenization temperatures (T_h) from 1150 to 1250 °C (Belkin et al., 1998; Lima et al., 2007). The homogenization temperature of the

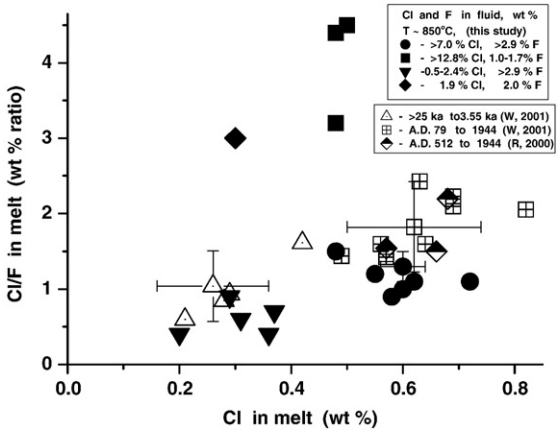

Fig. 5. The Cl/F ratios versus Cl contents of the melt measured in reheated clinopyroxene-hosted melt inclusions from Mt. Somma–Vesuvius rock samples (lava, scoria, pumice) and those from our experiments. *Open dotted triangles* are data for the eruptions from >25 ka to 3.55 ka (Webster et al., 2001). *Squares with crosses* are data for the eruptions from A.D. 79 to A.D. 1944 (Webster et al., 2001). *Half-filled diamonds* are data for the eruptions from A.D. 512 to A.D. 1944 (Raia et al., 2000). Symbols for our experiments are described in the legend. Error bars represent 1σ deviations.

phonolitic melt trapped in sanidine-hosted melt inclusions is around 850 °C. An equilibrium temperature of syn-eruptive mixing of magmas in shallow magma chamber for the A.D. 79 Plinian eruption of Vesuvius is estimated to be about 970 °C on the basis of mass and heat balance calculations (Cioni, 2000).

Webster and De Vivo (2002) clearly demonstrated that Cl concentration in Vesuvius magmas was dramatically enriched during evolution of the melt composition from phonotephrite through tephriphonolite to phonolite. In addition, the accumulation of volatiles in the residual melt could be enhanced by the crystallization of volatile-free minerals. These two factors might have forced the exsolution of hydrous Cl-bearing brines directly from the Cl-enriched magmas (Cioni, 2000; Webster and De Vivo, 2002; Webster, 2004; Webster and Mandeville, 2007).

Our experimental results can be used to discuss the role of fluid phase(s) in the evolution of Vesuvius phonolitic melts in a shallow magma chamber. The average Cl/F ratios versus ^{m}Cl in reheated silicate melt inclusions in clinopyroxene phenocrysts from Mt. Somma–Vesuvius samples and those from the experiments at ~850 °C are shown in Fig. 5. The eruptive products older than 3.55 ka are characterized by low Cl concentrations and low Cl/F ratios, similar to the experimental data obtained for Cl-poor and F-rich systems, indicating that those magmas were probably not saturated with respect to two fluid phases (low and high density phases). The glasses from the eruptions between A.D. 79 and A.D. 1944 have Cl contents above the maximum concentration which could be determined in phonolitic melts coexisting with two F-free or F-poor fluid phases (~0.5 wt% Cl; Fig. 1A and Signorelli and Carroll 2000). However, these natural glass compositions plot in the field obtained for melts coexisting with Cl-rich (>7 wt.%) and F-rich (>2.9 wt.%) experimental fluids (Fig. 5). Thus, if an exsolution of hydrosaline brines from the magma in Mt. Somma–Vesuvius occurred, as was proposed by Webster and De Vivo (2002) and Webster (2004), the concentrations of F in the brine and/or in the low-density fluid must have been relatively high. Future efforts should concentrate on the distribution of F between low and high density fluids to interpret the evolution of the fluid phase compositions in the phonolitic system of Mt. Somma–Vesuvius.

5. Conclusions

New experimental results on the solubility of mixed Cl- and F-bearing aqueous fluids in phonolitic melt and on the bulk fluid/melt partitioning provide a quantitative basis for an understanding of degassing processes in Cl- and F-rich evolved alkali-rich magmas. This study leads to several main observations, which were not demonstrated up to now. (1) The immiscibility gap between vapor and brine in Cl-rich systems is probably reduced by the presence of F in phonolitic systems. (2) For all experiments, $^{fl/m}D_F$ values >1 have been determined, indicating that fluorine is preferentially incorporated into the fluid phase in phonolitic systems. (3) The experiments confirm that Mt. Somma–Vesuvius phonolitic magmas from the eruptions between A.D. 79 and A.D. 1944 coexisted with Cl- and F-rich fluid(s) prior to eruption.

Acknowledgments

The authors are grateful to H. Behrens for assistance during experimental studies and the discussion of obtained results. We thank O. Diedrich and S. Schoenborn for the help with sample preparation and electron microprobe analyses, respectively. B. Scaillet and D. Dolejs are acknowledged for the very useful comments that improved the quality of the paper. Financial support was provided by the German Science Foundation (Ho 1337/8), the German Academic Exchange Service (DAAD study grant), Russian Foundation for Basic Research (Grant No.05-05-64754) and Scientific School (Grant No. NSh-3763.2008.5).

References

Anderko, A., Pitzer, K.S., 1993. Equation-of-state representation of phase equilibria and volumetric properties of the system NaCl–H_2O above 573 K. Geochim. Cosmochim. Acta 57, 1657–1680.
Behrens, H., 1995. Determination of water solubilities in high-viscosity melts: an experimental study on $NaAlSi_3O_8$ and $KAlSi_3O_8$ melts. Eur. J. Mineral. 7, 905–920.
Belkin, H.E., De Vivo, B., Torok, K., Webster, J.D., 1998. Pre-eruptive volatile content, melt-inclusion chemistry, and microthermometry of interplinian Vesuvius lavas (pre-A.D. 1631). J. Volcanol. Geotherm. Res. 82, 79–95.
Berndt, J., Liebske, C., Holtz, F., Freise, M., Nowak, M., Ziegenbein, D., Hurkuck, W., Koepke, J., 2002. A combined rapid-quench and H_2-membrane setup for internally heated pressure vessels: description and application for water solubility in basaltic melts. Am. Mineral. 87, 1717–1726.
Berndt, J., Koepke, J., Holtz, F., 2005. An experimental investigation of the influence of water and oxygen fugacity on differentiation of MORB at 200 MPa. J. Petrol. 46, 135–167.
Botcharnikov, R.E., Behrens, H., Holtz, F., Koepke, J., Sato, H., 2004. Sulfur and chlorine solubility in Mt. Unzen rhyodacitic melt at 850 °C and 200 MPa. Chem. Geol. 213, 207–225.
Botcharnikov, R.E., Holtz, F., Behrens, H., 2007. The effect of CO_2 on the solubility of H_2O–Cl fluids in andesitic melt. Eur. J. Mineral. 19, 671–680.
Candela, P.A., Piccoli, P.M., 1995. Model ore–metal partitioning from melts into vapor and vapor/brine mixtures. In: Thompson, J.F.H. (Ed.), Magmas, Fluids and Ore Deposits. Mineral. Assoc. Canada, pp. 107–127.
Carroll, M.R., 2005. Chlorine solubility in evolved alkaline magmas. Ann. Geophys. 48, 619–631.
Carroll, M.R., Blank, J.G., 1997. The solubility of H_2O in phonolitic melts. Am. Mineral. 82, 549–556.
Carroll, M.R., Webster, J.D., 1994. Solubilities of sulfur, noble gases, nitrogen, chlorine, and fluorine in magmas. In: Carroll, M.R., Holloway, J.R. (Eds.), Volatiles in Magmas, Rev. Mineral, vol. 30. Mineral. Soc. Am., Washington, pp. 231–279.
Chevychelov, V.Yu., 1999. Chlorine dissolution in fluid-rich granitic melts: the effect of calcium addition. Geochem. Intern. 37, 456–467.
Chevychelov, V.Yu., Chevychelova, T.K., 1997. Partitioning of Pb, Zn, W, Mo, Cl, and major elements between aqueous fluid and melt in the systems granodiorite (granite, leucogranite)–H_2O–NaCl–HCl. N. Jb. Mineral. Abh. 172, 101–115.
Chevychelov, V.Yu., Suk, N.I., 2003. Influence of the composition of magmatic melt on the solubility of metal chlorides at pressures of 0.1–3.0 kbar. Petrology 11, 62–74.
Chevychelov, V.Yu., Simakin, A.G., Bondarenko, G.V., 2003. Mechanism of chlorine dissolution in water-saturated model granodiorite melt: applications of IR spectroscopic methods. Geochem. Intern. 41, 395–409.
Chevychelov, V.Yu., Zaraisky, G.P., Borisovskii, S.E., Borkov, D.A., 2005. Effect of melt composition and temperature on the partitioning of Ta, Nb, Mn, and F between granitic (alkaline) melt and fluorine-bearing aqueous fluid: fractionation of Ta and Nb and conditions of ore formation in rare-metal granites. Petrology 13, 305–321.
Chevychelov, V.Yu., Botcharnikov, R.E., Holtz, F., 2008a. Experimental investigation of chlorine and fluorine contents in mica (biotite) and their partitioning between mica, phonolitic melt and fluid. Geochem. Intern. 46.
Chevychelov, V.Yu., Botcharnikov, R.E., Holtz, F., 2008b. Experimental investigation of chlorine and fluorine partitioning between fluid and subalkalic basaltic melt. Doklady Earth Sciences 422 (7), 1089–1092.
Chou, I.M., 1987. Phase relations in the system NaCl –KCl –H_2O: III. Solubilities of halite in vapor-saturated liquids above 445 °C and determinations of phase equilibrium properties in the system NaCl–H_2O to 1000 °C and 1500 bars. Geochim. Cosmochim. Acta 51, 1965–1975.
Christiansen, E.H., Lee, D.E., 1986. Fluorine and chlorine in granitoids from the basin and range province, western United States. Econ. Geol. 81, 1484–1494.
Cioni, R., 2000. Volatile content and degassing processes in the AD 79 magma chamber at Vesuvius (Italy). Contrib. Mineral. Petrol. 140, 40–54.
De Natale, G., Troise, C., Pingue, F., Mastrolorenzo, G., Pappalardo, L., 2006. The Somma–Vesuvius volcano (Southern Italy): structure, dynamics and hazard evaluation. Earth-Sci. Rev. 74, 73–111.
Devine, J.D., Gardner, J.E., Brack, H.P., Layne, G.D., Rutherford, M.J., 1995. Comparison of microanalytical methods for estimating H_2O contents of silicic volcanic glasses. Am. Mineral. 80, 319–328.
Dolejs, D., Baker, D.R., 2006. Fluorite solubility in hydrous haplogranitic melts at 100 MPa. Chem. Geol. 225, 40–60.
Dolejs, D., Baker, D.R., 2007a. Liquidus equilibria in the system K_2O–Na_2O–Al_2O_3–SiO_2–F_2O_{-1}–H_2O to 100 MPa: I. Silicate–fluoride liquid immiscibility in anhydrous systems. J. Petrol. 48, 785–806.
Dolejs, D., Baker, D.R., 2007b. Liquidus equilibria in the system K_2O–Na_2O–Al_2O_3–SiO_2–F_2O_{-1}–H_2O to 100 MPa: II. Differentiation paths of fluorosilicic magmas in hydrous systems. J. Petrol. 48, 807–828.
Dunbar, N.W., Hervig, R.L., Kyle, P.R., 1989. Determination of pre-eruptive H_2O, F and Cl contents of silicic magmas using melt inclusions: examples from Taupo volcanic center, New Zealand. Bull. Volcanol. 51, 177–184.
Freise, M., Holtz, F., Koepke, J., Scoates, J., Leyrit, H., 2003. Experimental constraints on the storage conditions of phonolites from the Kerguelen Archipelago. Contrib. Mineral. Petrol. 145, 659–672.
Gabitov, R.I., Price, J.D., Watson, E.B., 2005. Solubility of fluorite in haplogranitic melt of variable alkalis and alumina content at 800°–1000 °C and 100 MPa. Geochem. Geophys. Geosyst. 6, Q03007.
Glyuk, D.S., Trufanova, L.G., Bazarova, S.B., 1980. Phase relations in the granite–H_2O–LiF system at 1000 kg/cm^2. Geochem. Int. 17 (5), 35–48.
Gorbachev, N.S., Khodorevskaya, L.I., 1995. Partitioning of chlorine between aqueous fluid and basaltic melts at high pressures: behaviour of chlorine and water in processes of magma degassing. Dokl. Acad. Nauk 340 (5), 672–675 [in Russian].

Gramenitskiy, E.N., Shchekina, T.I., Deviatova, V.N., 2005. Phase Relations in the Fluorine-Bearing Granitic and Nepheline–Syenitic Systems and Partitioning of Elements Between Phases (Experimental Study). GEOS, Moscow. 188 p. [in Russian].
Hamilton, D.L., Henderson, C.M.B., 1968. The preparation of silicate compositions by a gelling method. Mineral. Mag. 36 (282), 832–838.
Harms, E., Schmincke, H.-U., 2000. Volatile composition of the phonolitic Laacher See magma (12,900 yr BP): implications for syn-eruptive degassing of S, F, Cl and H_2O. Contrib. Mineral. Petrol. 138, 84–98.
Heinrich, C.A., 2007. Fluid–fluid interactions in magmatic–hydrothermal ore formation. Rev. Mineral. Geochem. 65, 363–387.
Holtz, F., Dingwell, D.B., Behrens, H., 1993. Effects of F, B_2O_3, and P_2O_5 on the solubility of water in haplogranite melts compared to natural silicate melts. Contrib. Mineral. Petrol. 113, 492–501.
Holtz, F., Behrens, H., Dingwell, D.B., Johannes, W., 1995. H_2O solubility in haplogranitic melts: compositional, pressure, and temperature dependence. Am. Mineral. 80, 94–108.
Iacono Marziano, G., Schmidt, B.C., Dolfi, D., 2007. Equilibrium and disequilibrium degassing of a phonolitic melt (Vesuvius AD 79 "white pumice") simulated by decompression experiments. J. Volcanol. Geotherm. Res. 161, 151–164.
Keppler, H., 1993. Influence of fluorine on the enrichment of high field strength trace elements in granitic rocks. Contrib. Mineral. Petrol. 114, 479–488.
Keppler, H., Wyllie, P.J., 1991. Partitioning of Cu, Sn, Mo, W, U, and Th between melt and aqueous fluid in the systems haplogranite–H_2O–HCl and haplogranite–H_2O–HF. Contrib. Mineral. Petrol. 109, 139–150.
Kilinc, I.A., Burnham, C.W., 1972. Partitioning of chloride between a silicate melt and coexisting aqueous phase from 2 to 8 kilobars. Econ. Geol. 67, 231–235.
Koster van Groos, A.F., Wyllie, P.J., 1968. Melting relationships in the system $NaAlSi_3O_8$–NaF–H_2O to 4 kilobars pressure. J. Geol. 76, 50–70.
Koster van Groos, A.F., Wyllie, P.J., 1969. Melting relationships in the system $NaAlSi_3O_8$–NaCl–H_2O at one kilobar pressure, with petrological applications. J. Geol. 77 (5), 581–605.
Kotelnikova, Z.A., Kotelnikov, A.R., 2002. Synthetic NaF-bearing fluid inclusions. Geochem. Int. 40, 594–600.
Kovalenko, N.I., 1977. The reactions between granite and aqueous hydrofluoric acid in relation to the origin of fluorine-bearing granites. Geochem. Int. 14, 108–118.
Kravchuk, I.F., Keppler, H., 1994. Distribution of chloride between aqueous fluids and felsic melts at 2 kbar and 800 °C. Eur. J. Mineral. 6, 913–923.
Kravchuk, I.F., Slutsky, A.B., 2001. Behaviour of fluorine in fluid-magmatic system. Geokhimiya 6, 671–676 [in Russian].
Larsen, J.F., Gardner, J.E., 2004. Experimental study of water degassing from phonolite melts: implications for volatile oversaturation during magmatic ascent. J. Volcanol. Geotherm. Res. 134, 109–124.
Lima, A., De Vivo, B., Fedele, L., Sintoni, F., Milia, A., 2007. Geochemical variations between the 79 AD and 1944 AD Somma–Vesuvius volcanic products: constraints on the evolution of the hydrothermal system based on fluid and melt inclusions. Chem. Geol. 237, 401–417.
Lowenstern, J.B., 1994. Chlorine, fluid immiscibility, and degassing in peralkaline magmas from Pantelleria, Italy. Am. Mineral. 79, 353–369.
Lukkari, S., Holtz, F., 2007. Phase relations of a F-enriched peraluminous granite: an experimental study of the Kymi topaz granite stock, southern Finland. Contrib. Mineral. Petrol. 153, 273–288.
Malinin, S.D., Kravchuk, I.F., 1995. Behaviour of chlorine in silicate melt–aqueous chloride fluid equilibriums. Geokhimiya 8, 1110–1130 [in Russian].
Malinin, S.D., Kravchuk, I.F., Delbove, F., 1989. Chloride distribution between phases in hydrated and dry chloride–aluminosilicate melt systems as a function of phase composition. Geochem. Int. 26, 32–38.
Manning, D.A.C., 1981. The effect of fluorine on liquidus phase relationships in the system Qz–Ab–Or with excess water at 1 kbar. Contrib. Mineral. Petrol. 76, 206–215.
Marakushev, A.A., Gramenitskii, E.N., Korotaev, M.Yu., 1983. Petrological model of endogenic ore formation. Geol. Rudn. Mestorozd. 1, 3–20 [in Russian].
Marianelli, P., Métrich, N., Santacroce, R., Sbrana, A., 1995. Mafic magma batches at Vesuvius: a glass inclusion approach to the modalities of feeding stratovolcanoes. Contrib. Mineral. Petrol. 120, 159–169.
Marianelli, P., Métrich, N., Sbrana, A., 1999. Shallow and deep reservoirs involved in magma supply of the 1944 eruption of Vesuvius. Bull. Volcanol. 61, 48–63.
Mathez, E.A., Webster, J.D., 2005. Partitioning behavior of chlorine and fluorine in the system apatite–silicate melt–fluid. Geochim. Cosmochim. Acta 69, 1275–1286.
Métrich, N., Rutherford, M.J., 1992. Experimental study of chlorine behavior in hydrous silicic melts. Geochim. Cosmochim. Acta 56, 607–616.
Paone, A., Ayuso, R.A., De Vivo, B., 2001. A metallogenic survey of alkalic rocks of Mt. Somma–Vesuvius volcano. Mineral. Petrol. 73, 201–233.
Price, J.D., Hogan, J.P., Gilbert, M.C., London, D., Morgan, G.B., 1999. Experimental study of titanite–fluorite equilibria in the A-type Mount Scott Granite: implications for assessing F contents of felsic magma. Geol. 27 (10), 951–954.
Raia, F., Webster, J.D., De Vivo, B., 2000. Pre-eruptive volatile contents of Vesuvius magmas: constraints on eruptive history and behavior. I — The medieval and modern interplinian activities. Eur. J. Mineral. 12, 179–193.
Ravich, M.I., 1974. Water–Salt Systems at Elevated Temperatures and Pressures. Nauka, Moscow. 151 p. [in Russian].
Ravich, M.I., Valyashko, V.M., 1965. Solubility of sodium fluoride at elevated temperatures. Russ. J. Inorgan. Chem. 10, 107–109.
Roy, R., 1956. Aids in hydrothermal experimentation. J. Am. Ceram. Soc. 39, 145–146.
Santacroce, R., Bertagnini, A., Civetta, L., Landi, P., Sbrana, A., 1993. Eruptive dynamics and petrogenetic processes in a very shallow magma reservoir: the 1906 eruption of Vesuvius. J. Petrol. 34, 383–425.
Scaillet, B., Macdonald, R., 2003. Experimental constraints on the relationships between peralkaline rhyolites of the Kenya rift valley. J. Petrol. 44, 1867–1894.
Scaillet, B., Macdonald, R., 2004. Fluorite stability in silicic magmas. Contrib. Mineral. Petrol. 147, 319–329.
Schmidt, B.C., Behrens, H., 2008. Water solubility in phonolite melts, influence of melt composition and temperature. Chem. Geol. 256, 258–267 (this issue). doi:10.1016/j.chemgeo.2008.06.043.
Shinohara, H., 1994. Exsolution of immiscible vapor and liquid phases from a crystallizing silicate melt: implications for chlorine and metal transport. Geochim. Cosmochim. Acta 58, 5215–5221.
Shinohara, H., Iiyama, J.T., Matsuo, S., 1989. Partition of chlorine compounds between silicate melt and hydrothermal solutions. Geochim. Cosmochim. Acta 53, 2617–2630.
Signorelli, S., Capaccioni, B., 1999. Behaviour of chlorine prior and during the 79 A.D. Plinian eruption of Vesuvius (southern Italy) as inferred from the present distribution in glassy mesostases and whole-pumices. Lithos 46, 715–730.
Signorelli, S., Carroll, M.R., 2000. Solubility and fluid–melt partitioning of Cl in hydrous phonolitic melts. Geochim. Cosmochim. Acta 64, 2851–2862.
Signorelli, S., Carroll, M.R., 2002. Experimental study of Cl solubility in hydrous alkaline melts: constraints on the theoretical maximum amount of Cl in trachytic and phonolitic melts. Contrib. Mineral. Petrol. 143, 209–218.
Signorelli, S., Vaggelli, G., Romano, C., 1999. Pre-eruptive volatile (H_2O, F, Cl and S) contents of phonolitic magmas feeding the 3550-year old Avellino eruption from Vesuvius, southern Italy. J. Volcanol. Geotherm. Res. 93, 237–256.
Stelling, J., Botcharnikov, R.E., Beermann, O., Nowak, M., 2008. Solubility of H_2O- and Chlorine-bearing fluids in basaltic melt of Mount Etna at T=1050–1250 °C and P=200 MPa. Chem. Geol. 256, 101–109 (this issue). doi:10.1016/j.chemgeo.2008.06.043.
Straub, S.M., Layne, G.D., 2003. The systematics of chlorine, fluorine, and water in Izu arc front volcanic rocks: implications for volatile recycling in subduction zones. Geochim. Cosmochim. Acta 67, 4179–4203.
Thomas, R., Foerster, H.-J., Rickers, K., Webster, J.D., 2005. Formation of extremely F-rich hydrous melt fractions and hydrothermal fluids during differentiation of highly evolved tin–granite magmas: a melt/fluid-inclusion study. Contrib. Mineral. Petrol. 148, 582–601.
Thompson, A.B., Aerts, M., Hack, A.C., 2007. Liquid immiscibility in silicate melts and related systems. Rev. Mineral. Geochem. 65, 99–127.
Urusova, M.A., Ravich, M.I., 1966. Phase equilibria in the potassium fluoride–water system at elevated temperatures. Russ. J. Inorgan. Chem. 11, 353–357.
Veksler, I.V., 2004. Liquid immiscibility and its role at the magmatic–hydrothermal transition: a summary of experimental studies. Chem. Geol. 210, 7–31.
Webster, J.D., 1990. Partitioning of F between H_2O and CO_2 fluids and topaz rhyolite melt. Implications for mineralizing magmatic–hydrothermal fluids in F-rich granitic systems. Contrib. Mineral. Petrol. 104, 424–438.
Webster, J.D., 1992a. Fluid–melt interactions involving Cl-rich granites: experimental study from 2 to 8 kbar. Geochim. Cosmochim. Acta 56, 659–678.
Webster, J.D., 1992b. Water solubility and chlorine partitioning in Cl-rich granitic systems: effects of melt composition at 2 kbar and 800 °C. Geochim. Cosmochim. Acta 56, 679–687.
Webster, J.D., 1997a. Exsolution of magmatic volatile phases from Cl-enriched mineralizing granitic magmas and implications for ore metal transport. Geochim. Cosmochim. Acta 61, 1017–1029.
Webster, J.D., 1997b. Chloride solubility in felsic melts and the role of chloride in magmatic degassing. J. Petrol. 38, 1793–1807.
Webster, J.D., 2004. The exsolution of magmatic hydrosaline chloride liquids. Chem. Geol. 210, 33–48.
Webster, J.D., De Vivo, B., 2002. Experimental and modeled solubilities of chlorine in aluminosilicate melts, consequences of magma evolution, and implications for exsolution of hydrous chloride melt at Mt. Somma–Vesuvius. Am. Mineral. 87, 1046–1061.
Webster, J.D., Holloway, J.R., 1990. Partitioning of F and Cl between magmatic hydrothermal fluids and highly evolved granitic magmas. In: Stein, H.J., Hannah, J.L. (Eds.), Ore-bearing Granite Systems; Petrogenesis and Mineralizing Processes, Special Paper, vol. 246. Geol. Soc. Am., pp. 21–34.
Webster, J.D., Mandeville, C.W., 2007. Fluid immiscibility in volcanic environments. Rev. Mineral. Geochem. 65, 313–362.
Webster, J.D., Rebbert, C.R., 1998. Experimental investigation of H_2O and Cl solubilities in F-enriched silicate liquids; implications for volatile saturation of topaz rhyolite magmas. Contrib. Mineral. Petrol. 132, 198–207.
Webster, J.D., Kinzler, R.J., Mathez, E.A., 1999. Chloride and water solubility in basalt and andesite melts and implications for magmatic degassing. Geochim. Cosmochim. Acta 63, 729–738.
Webster, J.D., Raia, F., De Vivo, B., Rolandi, G., 2001. The behavior of chlorine and sulfur during differentiation of the Mt. Somma–Vesuvius magmatic system. Mineral. Petrol. 73, 177–200.